

Large Non-perturbative Effects of Small $m_{21}^2 = m_{31}^2$ and $\sin \theta_{13}$ on Neutrino Oscillation and CP Violation in Matter

Akira Takamura^{1,2} and Keiichi Kimura²

¹Department of Mathematics, Toyota National College of Technology
Eisei-cho 2-1, Toyota-shi, 471-8525, Japan

²Department of Physics, Nagoya University, Nagoya, 464-8602, Japan

Abstract

In the framework of three generations, we consider the CP violation in neutrino oscillation with matter effects. At first, we show that the non-perturbative effects of two small parameters, $m_{21}^2 = m_{31}^2$ and $\sin \theta_{13}$, become more than 50% in certain ranges of energy and baseline length. This means that the non-perturbative effects should be considered in detailed analysis in the long baseline experiments. Next, we propose a method to include these effects in approximate formulas for oscillation probabilities. Assuming the two natural conditions, $\theta_{23} = 45^\circ$ and matter density is symmetric, a set of approximate formulas, which involve the non-perturbative effects, has been derived in all channels.

1 Introduction

Last year, the direct evidence for neutrino oscillation [1] was found in three kinds of experiments, namely atmospheric neutrino experiment [2], reactor neutrino experiment [3] and K2K experiment [4]. In these experiments, the dip of neutrino oscillation, or the energy dependence, is observed. The possibilities of neutrino decay [5] and neutrino decoherence [6] are excluded by these results and it is found that the only solution for the solar and the atmospheric neutrino problem is neutrino oscillation. The observation of the dip also means that the neutrino experiments herald in a new era of precise measurements, because the effect, which disappears by averaging the energy and the baseline length, has been observed in these experiments for the first time.

From the results of the past experiments, it was found that the solar neutrino deficit is explained by the Large Mixing Angle MSW [7] solution [8, 9, 10],

$$m_{21}^2 \approx 8.3 \times 10^5 \text{ eV}^2; \quad \sin^2 2\theta_{12} \approx 0.8; \quad (1.1)$$

where the mass squared difference is defined by $m_{ij}^2 = m_i^2 - m_j^2$. It was obtained that

$$|m_{31}^2| \approx 2.0 \times 10^3 \text{ eV}^2; \quad \sin^2 2\theta_{23} \approx 1.0 \quad (1.2)$$

from the atmospheric neutrino experiment [11]. Furthermore, the upper bound of the 1-3 mixing angle, $\sin \theta_{13}$ is given by

$$\sin^2 2\theta_{13} \approx 0.2 \quad (1.3)$$

from the reactor experiment [12]. The next step for neutrino physics is the determination of $\sin \theta_{13}$, the sign of m_{31}^2 and CP phase δ . In particular, the measurement of the leptonic CP phase is one of the most important themes from the viewpoint of the origin of the universe. CP violation has been investigated also in quark sector for the first time and the Kobayashi-Maskawa theory has been established [13]. However, it has been found that the CP violation in quark sector is too small to generate the sufficient baryon number in the universe [14], because the electroweak symmetry breaking is not the first phase transition as the Higgs particle is too heavy. This means that the origin of Baryon Asymmetry of Universe is not CP violation from the KM phase and an extra source of CP violation is needed. One of the alternatives is the generation of baryon number due to the leptonic CP violation [15]. The possibility of this scenario has been investigated by many researchers.

In order to attain the next step, the long baseline experiments like superbeam experiments [16] and neutrino factory experiments [17] are planned. In these experiments, the earth matter effects disturb the observation of the CP violation because the matter in the earth is not CP invariant and generate the effects of fake CP violation. Therefore, it is very important to understand the earth matter effects in neutrino oscillation experiments.

Here, summarizing the results of the atmospheric, the solar and the reactor neutrino experiments, there are two small parameters as

$$\theta_{13} = \frac{m_{21}^2}{m_{31}^2} \approx 0.04; \quad (1.4)$$

$$s_{13} = \sin \theta_{13} \approx 0.23; \quad (1.5)$$

The magnitude of these parameters is the key for the observation of the leptonic CP violation because the CP violation cannot be observed in the limit of these parameters to zero. The largest value of θ_{13} has been chosen as the solution of the solar neutrino problem settled to the LMA MSW solution. If other solutions for the solar neutrino problem were chosen, the observation of the leptonic CP violation would be impossible in the earth experiments. This means that the LMA MSW solution opens the window for measuring the leptonic CP violation. However, if the value of s_{13} is too small, the observation of the CP violation will be impossible. The magnitude of s_{13} is one more key for our goal.

Let us briefly review the approximate formulas using the small parameter θ_{13} or s_{13} and the related papers. At first using the perturbation of oscillation probability in θ_{13} , the magnitude of the fake CP violation by the matter effects has been investigated in [18, 19, 20, 21, 22]. Furthermore by expanding the matter potential to the Fourier mode, it has been shown in [23, 24] that the mode with large wavelength mainly contributes to the oscillation probability. The higher order perturbative calculation has been done by [25, 26]. The perturbation in s_{13} has been investigated in [27]. The perturbation in both θ_{13} and s_{13} has also been studied in [28, 29]. This method has been extended to all channels in [30].

Next let us review the remarkable features related to the leptonic CP violation. In the case of constant matter density, the notable identity related to the leptonic CP violation has been found in [31, 32, 33]. In addition, it has been pointed out that the oscillation probability in matter almost coincide with that in vacuum under the certain condition, which is called vacuum mimicking phenomena, and the method to settle the fake CP violation by using the phenomena is discussed in detail [34, 35, 36]. Furthermore, it can be applied to the future long baseline experiments by using the statistical method [37, 38].

In the series of papers we have considered the three generation neutrino oscillation in matter and have shown that the CP dependence of the oscillation probabilities are derived exactly [39]. In the case that ν_e is included in the initial or final state, the CP dependence is given by

$$P(\nu_e \rightarrow \nu_e) = C_{ee}; \quad (1.6)$$

$$P(\nu_\mu \rightarrow \nu_\mu) = A \cos^2 + B \sin^2 + C; \quad (1.7)$$

and in the case that both the initial and final state are ν_μ ; ν_τ ; ν_τ , the CP dependence is given by

$$P(\nu_\mu \rightarrow \nu_\mu) = A \cos^2 + B \sin^2 + C + D \cos 2\theta + E \sin 2\theta; \quad (1.8)$$

where the coefficients A-E are independent of the CP phase. We have also shown that these coefficients can be calculated exactly in constant matter and then the approximate formulas are derived simply [40, 41]. Furthermore, we proposed a new method for approximating these coefficients in the case of non-constant matter density [42], and then applied it to the earth matter [43].

In this paper, we consider the two flavor neutrino oscillation. At first it has been shown that perturbation of the small mixing angle is not effective near the MSW resonance point. This means that the non-perturbative effects by the small mixing angle is important in the MSW resonance region. Next, we consider non-perturbative effects of $m_{21}^2 = m_{31}^2$ and $\sin \theta_{13}$ in the three generation neutrino oscillation. The importance of the non-perturbative effects is shown by comparing the exact numerical calculation with the perturbative expansion of the small parameters. Furthermore, we consider the method for deriving the approximate formulas in which the non-perturbative effects are taken into account. In our previous paper [42], the approximate formulas for $P(\nu_e \rightarrow \nu_\mu)$ have been derived. These formulas are effective for both MSW resonance regions. However, there is a problem because this method cannot be extended to other channels $P(\nu_\mu \rightarrow \nu_\mu)$ and so on. In order to solve this problem, we assume the two natural conditions, $\theta_{13} = 45^\circ$ and the symmetric matter potential. Under these conditions, we derive the approximate formulas for all channels, including non-perturbative effects of the two small parameters. These formulas are useful to discussing the problem of parameter degeneracy.

2 Non-perturbative Effect by Small Mixing Angle

In this section, we discuss the perturbative expansion of an small mixing angle in two generation neutrino oscillation. Then, we show that the perturbation breaks down in the MSW resonance region even if the mixing angle is small.

2.1 MSW Resonance of Probability in Two Generations

In this subsection, we consider the two generation neutrino oscillation and we choose the energy region and the baseline length in which the MSW resonance occurs. Let us start from the Hamiltonian in constant matter

$$H = O \text{diag}(0; \tilde{a}) O^T + \text{diag}(a; 0) \quad (2.1)$$

$$= \tilde{\sigma} \text{diag}(\tilde{m}_1; \tilde{m}_2) \tilde{\sigma}^T; \quad (2.2)$$

where the matter potential is defined by $a = \frac{P}{2} G_F N_e$. G_F is the Fermi constant and N_e is the electron density in matter. The matrix O is mixing matrix as

$$O = \begin{pmatrix} \cos \theta & \sin \theta \\ -\sin \theta & \cos \theta \end{pmatrix}; \quad (2.3)$$

where $\tilde{m}_i^2 = m_i^2 - 2E\tilde{a}$ and the quantities with tilde stand for the quantities in matter. Diagonalizing (2.1) to (2.2), effective masses \tilde{m}_i ($i = 1; 2$) and effective mixing angle $\tilde{\theta}$ are determined. If we use the notation $\tilde{\Delta} = \tilde{m}_2^2 - \tilde{m}_1^2$ as the mass squared difference, there is a relation between the mass squared difference and the mixing angles as

$$\tilde{\Delta} = \frac{\sin 2\tilde{\theta}}{\sin 2\theta} = \frac{\tilde{\Delta}}{\cos 2\theta} \frac{1}{\frac{a}{\tilde{\Delta}} + \sin^2 2\theta}; \quad (2.4)$$

Using these quantities in matter, the oscillation probability is given by

$$P = \sin^2 2\tilde{\theta} \sin^2 \frac{\tilde{\Delta} L}{2}; \quad (2.5)$$

The oscillating part with $L=E$ of this probability becomes large if the condition

$$\sin \frac{\tilde{\Delta} L}{2} \approx 1 \quad (2.6)$$

is satisfied. On the other hand, the condition for the maximum effective mixing angle is given by

$$\sin 2\tilde{\theta} \approx 1; \quad (2.7)$$

This condition is rewritten as $a = \frac{\tilde{\Delta}}{\cos 2\theta}$, and furthermore we define the resonance energy by

$$E = \frac{m^2}{2a}; \quad (2.8)$$

obtained from this condition. We also define the resonance length by

$$L = \frac{1}{a \sin \theta}; \quad (2.9)$$

The energy and the baseline length are determined, if the two conditions (2.8) and (2.9) are both satisfied. We define this point in $E-L$ space as the resonance point. The position of the resonance point is determined by three quantities, the mass squared difference m^2 , the matter potential a and the small mixing angle $\sin \theta$ as seen from (2.8) and (2.9).

2.2 Perturbation due to Small Mixing Angle

Next, let us consider the expansion of the effective mass \tilde{m} and the effective mixing angle $\sin 2\tilde{\theta}$ by small mixing angle $\sin \theta$. We show that although the effective mass and the effective mixing angle diverge in the MSW resonance energy, the oscillation probability, the function of these two quantities, converges.

At first, the effective mass is expanded as

$$\tilde{m} = j \left[a_j + \frac{2a}{j} \frac{\sin^2 \theta}{a_j} + \frac{a^2}{2j} \frac{\sin^4 \theta}{a_j^2} + \dots \right] \quad (2.10)$$

One can see from this result that the other terms than the first term diverge. The higher order terms have larger divergence near the MSW resonance. The effective mixing angle is expanded as

$$\sin 2\tilde{\theta} = \frac{\sin 2\theta}{j} \left[1 - \frac{2a}{j} \frac{\sin^2 \theta}{a_j} + \frac{3a^2}{2} \frac{\sin^4 \theta}{a_j^2} + \dots \right] \quad (2.11)$$

The condition

$$\sin \theta < \frac{j}{2} \frac{a_j}{a} \quad (2.12)$$

is needed for $\sin 2\tilde{\theta}$ to converge to a finite value. However, this condition cannot be satisfied in the MSW resonance defined by $\frac{2a}{j} \frac{\sin^2 \theta}{a_j} = 1$, even if $\sin \theta$ is small. This means that the above perturbation becomes a divergence series. In the expansion for the effective mass and the effective mixing angle, the coefficients become large even if these quantities are expanded by the small mixing angle.

Next, let us consider the oscillation probability and let us demonstrate that the oscillation probability takes the finite value, where the divergences due to the effective mass and the effective mixing angle are canceled out each other. Substituting (2.10) and (2.11) into (2.5), we obtain

$$P = \frac{\sin^2 2\tilde{\theta}}{4} \sin^2 \left(\frac{a}{2} L \right) + \frac{\sin^2 2\tilde{\theta}}{4} \frac{4a}{j} \frac{\sin^2 \theta}{a_j} \sin^2 \left(\frac{a}{2} L \right) + \frac{a}{a} L \frac{\sin^2 \theta}{a} \sin \left(\frac{a}{2} L \right) + \dots \quad (2.13)$$

In the limit, $a \rightarrow \infty$, it is found that the oscillation probability becomes finite as

$$P = \lim_{a \rightarrow \infty} \frac{\sin^2 2\tilde{\theta}}{4} \sin^2 \left(\frac{a}{2} L \right) + \lim_{a \rightarrow \infty} \frac{\sin^2 2\tilde{\theta}}{4} \frac{4a}{j} \frac{\sin^2 \theta}{a_j} \sin^2 \left(\frac{a}{2} L \right) + \frac{a}{a} L \frac{\sin^2 \theta}{a} \sin \left(\frac{a}{2} L \right) + \dots \quad (2.14)$$

$$= \cos^2 \theta \sin^2 \theta a^2 L^2 - \frac{1}{3} \sin^4 \theta a^4 L^4 + \dots \quad (2.15)$$

From this equation, the oscillation probability becomes finite as the divergences due to the effective mass and the effective mixing angle are canceled out each other. However, there is a difference between this finite value and the exact one. In order to understand this fact, we should take the limit, $a \rightarrow \infty$, directly in the expression (2.5) of the exact oscillation probability. Then, we obtain

$$P = \lim_{a \rightarrow \infty} \frac{\sin^2 2\theta}{4} \sin^2 \left(\frac{a}{2} L \right) \frac{1}{(\cos^2 \theta + 4a \sin^2 \theta)^2} \quad (2.16)$$

$$= \cos^2 \theta \sin^2 \theta (\sin aL)^2 \quad (2.17)$$

Comparing these two results, (2.15) and (2.17), the shorter the baseline length L is, the smaller the difference becomes. Namely, the condition for the perturbation to be a good approximation is

$$a \sin L < 1 \quad (2.18)$$

We rewrite this condition as

$$L < \frac{1}{a \sin \theta} \quad (2.19)$$

As you see from (2.9), this is the condition that the baseline length is shorter than the resonance length.

Next, let us investigate the magnitude of non-perturbative effects numerically. We use the following parameters, $m^2 = 2:0 \cdot 10^3 \text{ eV}^2$ and $\sin \theta = 0:16$. We set the baseline length, $L = 6000 \text{ km}$ and the energy region, $1 \text{ GeV} \leq E \leq 50 \text{ GeV}$, to include the MSW resonance energy. Furthermore we choose the density $\rho = 4 \text{ g/cm}^3$.

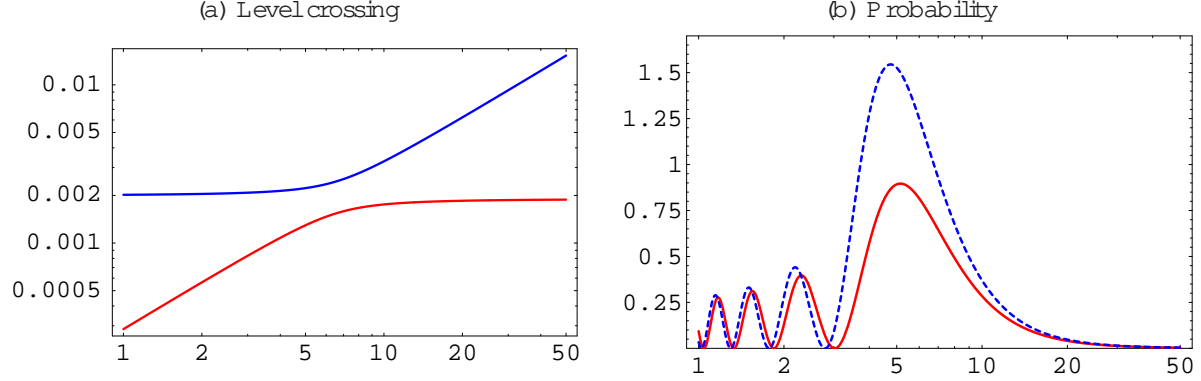


Figure 1: Comparison of the perturbative value with the exact one in the two generation neutrino oscillation probability. In (a), the energy dependence of two eigenvalues is plotted. In (b), the dotted and solid line show the values by the perturbative and numerical calculations, respectively.

At first, in figure 1(a) it is plotted the level crossing of two eigenvalues. It is shown that the crossing energy is about 6-7 GeV and corresponds to the MSW resonance energy. Next in figure 1(b), we compare the oscillation probability calculated by perturbation with the one by numerical calculation. These figures show that the perturbation breaks down around the MSW resonance energy. Summarizing the results of this subsection,

1. The perturbative expansion in the small mixing angle breaks down around the MSW resonance because the perturbation becomes the divergent series. The coefficients of this expansion become larger around the MSW resonance. The divergence included in the effective mass cancels with that in the effective mixing angle, and as a result, the value of the oscillation probability takes finite value. This cancellation occurs order by order.
2. Although the divergences of the effective mass and the effective mixing angle in the perturbative expansion cancel in the oscillation probability, the finite value of the probability differs from that by numerical calculation. Although the perturbation around the MSW resonance energy becomes a good approximation if the baseline length is shorter than the resonance length as seen from (2.19), we need to take higher order terms of perturbation into account in the longer baseline length, namely non-perturbative effects are important there.

3 New Idea to Approximate Oscillation Probabilities

In this section, we consider the matter effects in three generation neutrino oscillation. At first, we review that the 2-3 mixing angle θ_{23} and the CP phase δ can be separated from matter effects in the oscillation probability [39]. This means that the matter effects appear through the remained four parameters. Furthermore, these four parameters can be separated to two set of parameters and each set is related to the phenomena in low and high energy as

$$(\theta_{12}; m_{21}^2) : \text{Low Energy Phenomenon} \quad (3.1)$$

$$(\theta_{13}; m_{31}^2) : \text{High Energy Phenomenon} \quad (3.2)$$

This separation means that the parameters for the solar neutrino and those for the atmospheric neutrino are almost independent each other. We propose the method deriving the approximate formulas simply by using this feature.

3.1 Definition of Low and High Energy Regions

In this subsection, we define the low energy and the high energy Hamiltonians by taking the limit of small quantity like s_{13} or θ to zero.

It is noted that $H(t)$ satisfies the relation

$$H(t) = O_{23} H^0(t) O_{23}^T \quad (3.3)$$

where H^0 is given by

$$H^0 = O_{13} O_{12} \text{diag}(0; \theta_{21}; \theta_{31}) O_{12}^T O_{13}^T + \text{diag}(a(t); 0; 0) \quad (3.4)$$

This means that the 1-2 and 1-3 mixing angles are separated from the 2-3 mixing and the CP phase. See Appendix A for the detailed calculation. In this Appendix A, we derive the same result as that derived from this section from another point of view. Taking the limit $s_{13} \rightarrow 0$, the Hamiltonian reduces to the two generation Hamiltonian as

$$H^l = \lim_{s_{13} \rightarrow 0} H^0 \quad (3.5)$$

$$= O_{12} \text{diag}(0; \theta_{21}; \theta_{31}) O_{12}^T + \text{diag}(a(t); 0; 0) \quad (3.6)$$

$$= \begin{pmatrix} \theta_{21} s_{12}^2 + a(t) & \theta_{21} s_{12} c_{12} & 0 \\ \theta_{21} s_{12} c_{12} & \theta_{21} c_{12}^2 & 0 \\ 0 & 0 & \theta_{31} \end{pmatrix} A \quad (3.7)$$

This means that the third generation is separated from the first and the second generation. As seen from this Hamiltonian (3.7), the components except for H^l , depend only on $(\theta_{12}; \theta_{21})$. We call H^l the low energy Hamiltonian. On the other hand, taking the limit $\theta \rightarrow 0$, the Hamiltonian reduces to the two generation Hamiltonian as

$$H^h = \lim_{\theta \rightarrow 0} H^0 \quad (3.8)$$

$$= O_{13} \text{diag}(0; 0; \theta_{31}) O_{13}^T + \text{diag}(a(t); 0; 0) \quad (3.9)$$

$$= \begin{pmatrix} \theta_{31} s_{13}^2 + a(t) & 0 & \theta_{31} s_{13} c_{13} \\ 0 & 0 & 0 \\ \theta_{31} s_{13} c_{13} & 0 & \theta_{31} c_{13}^2 \end{pmatrix} A \quad (3.10)$$

This means that the second generation is separated from the first and the third generations. This Hamiltonian (3.10) is expressed by only the parameters $(\theta_{13}; \theta_{31})$. We call H^h high energy Hamiltonian. Next, let us define high and low energy regions described by H^h and H^l . We first calculate the MSW resonance energy because the MSW effect is the most important in matter effects. In the case of $L = 6000 \text{ km}$, which we use later, the average matter potential is calculated as $\rho = 3.91 \text{ g/cm}^3$. By using this value, we obtain the high energy MSW resonance as

$$E^h = m_{31}^2 = a \approx 5 \text{ GeV} \quad (3.11)$$

and the low energy MSW resonance as

$$E^l = m_{21}^2 = a \approx 0.2 \text{ GeV} \quad (3.12)$$

From these results, we regard $E = 1 \text{ GeV}$ as the boundary energy of low and high energy regions. Therefore, we define the high and the low energy regions as

$$E < 1 \text{ GeV} : \text{Low Energy Region} \quad (3.13)$$

$$E > 1 \text{ GeV} : \text{High Energy Region} \quad (3.14)$$

3.2 Order Counting of Amplitude on θ and s_{13}

In this subsection, we investigate how the amplitude S^0 depends on the two small parameters θ and s_{13} . Then, we clarified the general features of S^0 related to the order of θ and s_{13} .

At first, we represent the explicit form of the Hamiltonian factored out the 2-3 mixing angle and the CP phase as

$$H^0(t) = O_{13} O_{12} \text{diag}(0; \quad \quad \quad) O_{12}^T O_{13}^T + \text{diag}(a(t); 0; 0) \quad (3.15)$$

$$= \begin{pmatrix} 21 C_{13}^2 s_{12}^2 + 31 s_{13}^2 + a(t) & 21 C_{13} s_{12} C_{12} & 21 C_{13} s_{13} s_{12}^2 + 31 s_{13} C_{13} \\ 21 C_{13} s_{12} C_{12} & 21 C_{12}^2 & 21 s_{13} s_{12} C_{12} \\ 21 C_{13} s_{13} s_{12}^2 + 31 s_{13} C_{13} & 21 s_{13} s_{12} C_{12} & 21 s_{13}^2 s_{12}^2 + 31 C_{13}^2 \end{pmatrix} A : \quad (3.16)$$

The components of this Hamiltonian depends on θ and s_{13} as

$$H^0(t) = \begin{pmatrix} 0 & O(1) & O(\theta) & O(s_{13}) \\ O(\theta) & O(\theta) & O(\theta) & O(s_{13}) \\ O(s_{13}) & O(s_{13}) & O(s_{13}) & O(1) \end{pmatrix} A : \quad (3.17)$$

From this result, we can see that non-diagonal components are small compared with diagonal components. We also understand that H^0 is the smallest component and H_e^0 ; H_s^0 are next smaller component. We should note the salient feature that the result of this order counting holds in H^n for arbitrary n . Namely, we obtain

$$(H^0(t))^n = \begin{pmatrix} 0 & O(1) & O(\theta) & O(s_{13}) \\ O(\theta) & O(\theta^2) & O(\theta) & O(s_{13}) \\ O(s_{13}) & O(s_{13}) & O(\theta) & O(1) \end{pmatrix} A \quad \text{for } n = 1; 2; \dots : \quad (3.18)$$

As this result, the order of the amplitude $S^0(t)$ for two small parameters θ and s_{13} is given by

$$S^0(t) = T \exp \int_0^t i H^0(t) dt = \begin{pmatrix} 0 & O(1) & O(\theta) & O(s_{13}) \\ O(\theta) & O(1) & O(s_{13}) & \\ O(s_{13}) & O(s_{13}) & O(1) & \end{pmatrix} A : \quad (3.19)$$

This result is almost the same as that of the original Hamiltonian. Furthermore, we consider the general features derived from the original Hamiltonian. The s_{13} dependence of this Hamiltonian is described as

$$H^0 = \begin{pmatrix} \text{even} & \text{even} & \text{odd} \\ \text{even} & \text{even} & \text{odd} \\ \text{odd} & \text{odd} & \text{even} \end{pmatrix} A : \quad (3.20)$$

This dependence does not change for $(H^0)^n$ as

$$(H^0)^n = \begin{pmatrix} \text{even} & \text{even} & \text{odd} \\ \text{even} & \text{even} & \text{odd} \\ \text{odd} & \text{odd} & \text{even} \end{pmatrix} A \quad \text{for } n = 1; 2; \dots : \quad (3.21)$$

As this result, the amplitude $S^0(t)$ has the same structure,

$$S^0 = T \exp \int_0^t i H^0(t) dt = \begin{pmatrix} \text{even} & \text{even} & \text{odd} \\ \text{even} & \text{even} & \text{odd} \\ \text{odd} & \text{odd} & \text{even} \end{pmatrix} A : \quad (3.22)$$

This is the general feature which holds in arbitrary matter profile.

3.3 Proposal of Simple Method

In the previous subsection, we have shown the general features (3.19) and (3.22) of the amplitude $S^0(t)$ related to the two small parameters s_{13} and θ . However, we cannot calculate $S^0(t)$ by using only this features. In this subsection, we propose the concrete method for the calculation. Let us consider if there is the approximation available both in low and high energy. After expanding the amplitude S^0 on the two small parameters θ and s_{13} , we can arrange this as

$$S^0 = O(1) + O(\theta) + O(s_{13}) + O(\theta^2) + O(s_{13}) + O(s_{13}^2) + \dots \quad (3.23)$$

$$= O(1) + O(\theta) + O(\theta^2) + \dots + O(1) + O(s_{13}) + O(s_{13}^2) + \dots + O(1) + O(s_{13}) + O(\theta^2 s_{13}) + O(s_{13}^2) + \dots \quad (3.24)$$

$$= \lim_{s_{13} \rightarrow 0} S^0 + \lim_{\theta \rightarrow 0} S^0 - \lim_{s_{13} \rightarrow 0} S^0 + O(s_{13}) + O(\theta^2 s_{13}) + \dots \quad (3.25)$$

$$= S^{\theta} + S^{s_{13}} - S^{\theta, s_{13}} + O(s_{13}) + O(\theta^2 s_{13}) + O(s_{13}^2) + \dots ; \quad (3.26)$$

where S^0 ; S^h and S^d are defined by

$$S^0 = \lim_{s_{13} \rightarrow 0} S^0 = T \exp \int_0^Z i H^0 dt \quad (3.27)$$

$$S^h = \lim_{s_{13} \rightarrow 0} S^0 = T \exp \int_0^Z i H^h dt \quad (3.28)$$

$$S^d = \lim_{s_{13} \rightarrow 0} S^0 = \text{diag} \exp \int_0^Z i a(t) dt ; 1; e^{i s_{13} L} ; \quad (3.29)$$

respectively. S^0 (S^h) corresponds to the amplitudes, which gives the main contribution in low (high) energy. S^d is the double counting term because the contribution of this term is included both from low energy and high energy terms. Therefore, we subtract this contribution and approximate the amplitude as

$$S^0 \approx S^0 + S^h - S^d \quad (3.30)$$

ignoring higher order terms. Let us discuss this approximation which is used to derive our main result here.

In (3.23)–(3.26), the higher order terms in ϵ and s_{13} are included in S^0 and S^h . The reason for including the higher order terms is to take into account non-perturbative effects, which become important in the low and high energy MSW resonance region as discussed in section 2. On the other hand, we ignore the higher order terms, which are proportional to both ϵ and s_{13} . If the second order of small parameters, ϵ^2 and s_{13}^2 , is considered as an example, we ignore only $O(\epsilon^2)$ term in three terms with order $O(\epsilon^2)$; $O(s_{13}^2)$ and $O(\epsilon s_{13})$. This procedure is more appropriate than usual perturbation because both non-perturbative effects on small ϵ in low energy region and on small s_{13} in high energy region can be taken in our approximation. However, as the derivation of the approximation (3.30) is not exact, we need to numerically check this later. In the previous subsection, the parity of the matrix elements related to s_{13} has been derived. The equations (3.19), (3.22) and (3.30) lead to the magnitude of the correction for the amplitudes as

$$S_e^0 = S_e^0 + O(s_{13}^2) \quad (3.31)$$

$$S_e^0 = S_e^h + O(s_{13}) \quad (3.32)$$

$$S^0 = O(s_{13}) \quad (3.33)$$

$$S_{ee}^0 = S_{ee}^0 + S_{ee}^h - S_{ee}^d + O(s_{13}^2) \quad (3.34)$$

$$S^0 = S^0 + O(s_{13}^2) \quad (3.35)$$

$$S^0 = S^h + O(s_{13}^2) \quad (3.36)$$

If we ignore the higher order terms which are proportional to both ϵ and s_{13} in these equations, we obtain approximate formulas by using the two generation amplitudes. The main term for S_e^0 ; S^0 is approximated by the low-energy amplitude as seen from (3.31) and (3.35). On the other hand, the main term for S_e^0 and S^0 are approximated by the high-energy amplitude as seen from (3.32) and (3.36). These features come from the eq. (3.19). As seen from (3.31)–(3.36), these are expressed by only two generation amplitudes and have an advantage for their simple form. The precision of the approximation depends on the values of s_{13} and ϵ . If the value of s_{13} is smaller than the upper bound derived by the CHOOZ experiment, the precision of approximation becomes better. It is noted that the method described in this subsection does not need the assumption for the matter density to be constant.

Next, we show that the approximate formulas (3.31)–(3.36) coincide with the numerical calculation with a good precision. We choose the Preliminary Reference Earth Model (PREM) as an earth matter density model and compare the amplitudes in all channels calculated from our approximate formulas with the numerical calculation. Here, $m_{21}^2 = 8.3 \times 10^5 \text{ eV}^2$; $m_{31}^2 = 2.0 \times 10^3 \text{ eV}^2$; $\sin^2 2\theta_{12} = 0.8$ and $\sin^2 \theta_{13} = 0.23$ are chosen. Furthermore, we set the baseline length as $L = 6000 \text{ km}$, where the MSW effect becomes large, and the energy region as $1 \text{ GeV} < E < 20 \text{ GeV}$, where the MSW resonance energy is included.

We compare our formulas with the numerical calculation in Figure 2. One can see that there are some features in the following. At first, four amplitudes \mathcal{P}_e^0 ; \mathcal{P}_{ee}^0 ; \mathcal{P}^0 and \mathcal{P}^0 coincide with the numerical calculation with a good precision. This is because there is not the first order correction of s_{13} from (3.31) and (3.34)–(3.36). Next the low-energy part of \mathcal{P}_e^0 is different from the numerical calculation a little. This is understood from the eq. (3.32). Furthermore our approximation in \mathcal{P}^0 is not agreement with numerical calculation at all. Although the value of this amplitude is exactly zero in our approximation as seen from (3.33), the actual magnitude of this amplitude attains 0.02 in low energy from Figure 1. It is

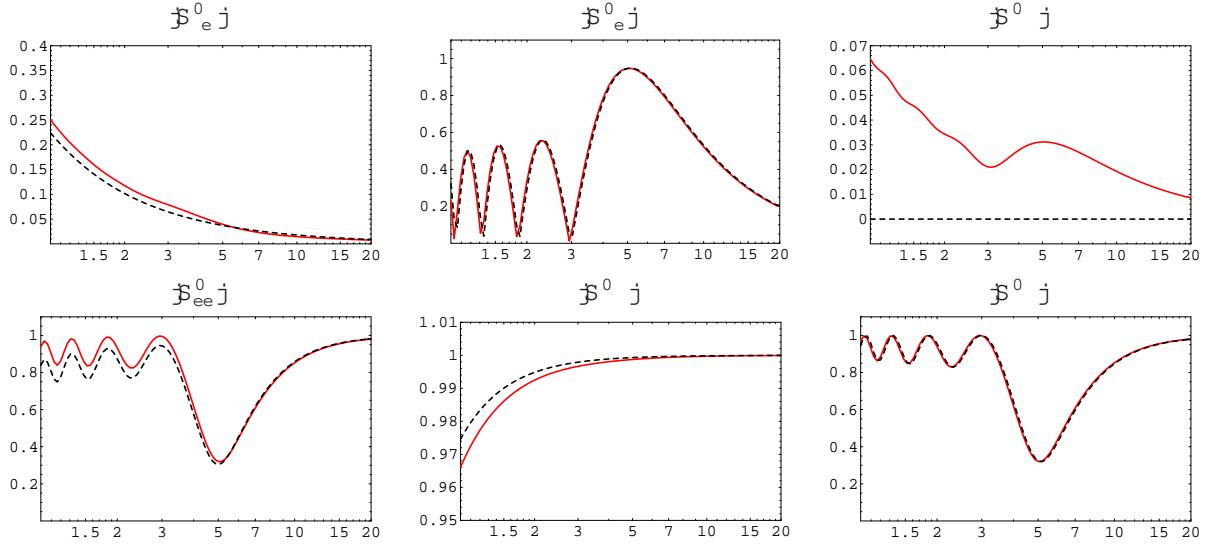


Figure 2: Comparison of our approximate formulas with the numerical calculation. In these figures the absolute value of the amplitudes in all channels is plotted to compare our formulas with numerical calculation. The solid lines show the approximate probabilities calculated from (3.31)–(3.36) and the dashed lines show the probabilities in the numerical calculation.

noted that this value is almost same as the value expected from the order counting $O(s_{13}) \approx 0.01$. Next we would like to derive the approximate formulas of the oscillation probabilities from the amplitudes obtained here. However, there is a problem. As seen from eqs. (A.32)–(A.49) in Appendix A, we cannot obtain the approximate formulas for the CP dependence of the probabilities $P(\mu \rightarrow \mu)$; $P(\mu \rightarrow e)$ and $P(\mu \rightarrow \tau)$. The reason is that the CP dependence in these channels is directly proportional to S^0 . Although it does not seem to proceed the calculation, there is a method to indirectly calculate the CP dependence of these three channels by using unitarity even if we cannot directly obtain the amplitude S^0 , as we show in sec. 4.

3.4 Discussion

In this subsection, let us reconsider the method proposed in the previous subsection in more detail. In (3.23)–(3.26), we ignore the terms of order $O(s_{13})$ for the amplitude S^0 . The readers wonder if we ignore the terms of order $O(s_{13})$ for a quantity other than amplitude S^0 , for example H^0 and P . Here, let us demonstrate the case of using the physical quantity, H^0 or P as Q . Expanding Q on s_{13} , we obtain

$$Q = Q' + Q^h - Q^d + O(s_{13}) + O(s_{13}^2) + \dots \quad (3.37)$$

by the same procedure as (3.23)–(3.26). If we neglect the higher order terms like $O(s_{13})$, we can approximate Q as

$$Q \approx Q' + Q^h - Q^d \quad (3.38)$$

As the case of the approximated amplitude defined in the previous subsection, $Q' = Q'(12; 21)$ is the main term in low-energy and $Q^h = Q^h(13; 31)$ is the main term in high-energy. Q^d is the double counting term. This method for the approximation is new from the view point that it takes into account non-perturbative effects by both the two MSW resonance. This method is effective whatever we choose the quantity Q in principle, but there is a difference for the simplicity and the magnitude of error, as discussed below.

We consider the Hamiltonian H^0 as Q . Namely, H^0 can be approximated as

$$H^0 \approx H' + H^h - H^d; \quad (3.39)$$

where double counting term is given by

$$H^d = \text{diag}(a(t); 0; 31); \quad (3.40)$$

There is the problem for the simplicity in this approximation. Because the form of the solution for the amplitude is given by

$$S^0 = T \exp \int_0^Z (H^{\prime} + H^h - H^d) dt ; \quad (3.41)$$

and we cannot simplify this amplitude without calculation of the commutator of H^{\prime} and H^h . This means that direct application of our method for the Hamiltonian needs another approximation to estimate the amplitude and is not effective from the point of the simplicity. Namely, the amplitudes can not be calculated within the framework of two generation approximation although the precision of this approximation has a good.

Next, let us consider the probability P as the quantity Q . In this case, we can approximate as

$$P = P^{\prime} + P^h - P^d ; \quad (3.42)$$

where P^{\prime} and P^h are given by

$$P^{\prime(h)} = T \exp \int_0^Z i H^{\prime(h)} dt ; \quad (3.43)$$

and P^d is the identity matrix. As an example, we consider $P(e \rightarrow \mu)$. The CP phase dependence is given by

$$P(e \rightarrow \mu) = A_e \cos \delta + B_e \sin \delta + C_e ; \quad (3.44)$$

where the coefficients A_e and B_e determines the magnitude of the CP violation. On the other hand, the CP violation becomes zero in the limit, $\delta \rightarrow 0$ or $s_{13} \rightarrow 0$, as seen from

$$A_e = O(s_{13}); \quad B_e = O(s_{13}); \quad (3.45)$$

Namely, we obtain

$$A_e^{\prime} = A_e^h = A_e^d = 0; \quad B_e^{\prime} = B_e^h = B_e^d = 0 \quad (3.46)$$

and we cannot calculate the quantities like the CP violation, which includes the effect in three generations, in this approximation. This result holds for all channels.

To summarize this subsection, if we choose the Hamiltonian H^0 as Q , the precision of approximation is good, but the calculation is not so simple compared to the exact calculation. If we choose the probability P as Q , we cannot calculate the three generation effects like CP violation. On the other hand, if we choose the amplitude S^0 as Q , we can calculate the three generation effects like CP violation within the framework of two generation approximation.

4 Approximate Formulas for Oscillation Probabilities

In this section, we calculate the matrix elements, not determined by the method in the previous section, by using the unitarity. After that, we derive the approximate formulas of the oscillation probabilities $P(\nu_i \rightarrow \nu_j)$ in arbitrary matter profile without using S^0 directly. Namely, we derive the approximate formulas in all channels by our new method.

4.1 Unitarity Relation

We cannot calculate the amplitude S^0 in the method introduced in the previous section. The reason is that the amplitude S^0 is a very small quantity, which has an order of $O(s_{13})$. As seen from (A.32)–(A.49) in Appendix A, it seems that the approximate formulas, including CP violation, of three channels, $P(\nu_e \rightarrow \nu_\mu)$; $P(\nu_e \rightarrow \nu_\tau)$ and $P(\nu_\mu \rightarrow \nu_\tau)$ cannot be derived without directly calculating the amplitude S^0 . However in this subsection, we can derive these probabilities without directly calculating this amplitude if we assume the two natural conditions,

$$s_{23} \ll c_{23}; \quad (4.1)$$

$$s^0 \ll s^0; \quad (4.2)$$

The first condition is supported by best fit value of the atmospheric neutrino experiments and the second condition holds in one-dimensional model of the earth matter density like the PREM and ak-135f. Accordingly, the error due to the difference between these conditions and the real situations is considered to be relatively small. We proceed the analysis under these two conditions in the following.

At first, we obtain

$$B = 2\text{Im} [(S^0 c_{23}^2 + S^0 s_{23}^2) (S^0 - S^0)] c_{23} s_{23} = 0 \quad (4.3)$$

from (A.34) and (4.2) in the case of the symmetric matter density. In the same way, we obtain

$$B = 2\text{Im} [(S^0 s_{23}^2 + S^0 c_{23}^2) (S^0 - S^0)] c_{23} s_{23} = 0 \quad (4.4)$$

from (A.40) and (4.2). Furthermore, in the case of the symmetric matter density and the maximal $2-3$ mixing angle 45° , we also obtain

$$A = 2\text{Re}[(S^0 - S^0) (S^0 c_{23}^2 - S^0 s_{23}^2)] c_{23} s_{23} = 0 \quad (4.5)$$

from (A.45) and (4.2). Let us here consider how the oscillation probabilities, related with the amplitude S^0 and not determined in the previous section, are derived. At first, in the probability,

$$P(\nu_e \rightarrow \nu_e) = A \cos^2 + B \sin^2 + C + D \cos 2\theta + E \sin 2\theta; \quad (4.6)$$

the coefficient proportional to \cos^2 can be calculated as

$$A = A_e - A' - A_e' - 2\text{Re}[S_e^h S_e^h] s_{23} c_{23} \quad (4.7)$$

from (4.5) and the unitarity relation. Next, let us turn to the probability $P(\nu_e \rightarrow \nu_\mu)$. In the probability,

$$P(\nu_e \rightarrow \nu_\mu) = A \cos^2 + B \sin^2 + C + D \cos 2\theta + E \sin 2\theta; \quad (4.8)$$

the coefficient of \cos^2 can be calculated as

$$A = A_e - A' - A_e' - 2\text{Re}[S_e^h S_e^h] s_{23} c_{23} \quad (4.9)$$

from (4.5) and the unitarity relation.

Finally, let us calculate the probability $P(\nu_e \rightarrow \nu_\tau)$. In the probability,

$$P(\nu_e \rightarrow \nu_\tau) = A \cos^2 + B \sin^2 + C + D \cos 2\theta + E \sin 2\theta; \quad (4.10)$$

the coefficient of \sin^2 becomes

$$B = B_e - B' - B_e' - 2\text{Im}[S_e^h S_e^h] s_{23} c_{23} \quad (4.11)$$

from (4.3) and the unitarity relation. We can derive the probability up to the second order of two small parameters by using the unitarity relation although we cannot directly calculate S^0 in the previous method. In addition, the coefficients of $\sin 2\theta$ and $\cos 2\theta$, D and E , have an order of

$$D = O(\theta^2 s_{13}^2); \quad E = O(\theta^2 s_{13}^2) \quad (4.12)$$

in these three channels from (A.36), (A.37), (A.42), (A.43), (A.48) and (A.49) and are expected to be small. Actually, these coefficients have the second order of S^0 , and the values are about $(0.02)^2 \sim 0.0004$ from Figure 1 in high energy region related with long baseline experiments. So we ignore them in the following section.

4.2 Approximate Formulas in All Channels

In this subsection, we present the approximate formulas which is useful in arbitrary matter density profile. Ignoring the higher order terms of θ and s_{13} than the second order, we can present the oscillation probabilities for all channels with the amplitudes calculated in two generations.

At first, let us derive the approximate formulas for $P(\nu_e \rightarrow \nu_e)$ and $P(\nu_e \rightarrow \nu_\mu)$. We only have to replace the amplitudes S_e^0 and S_e^h in three generations into S_e^l and S_e^h in two generations. From (A.24)–(A.31) and (3.31)–(3.32), we obtain

$$P(\nu_e \rightarrow \nu_e) = A_e \cos^2 + B_e \sin^2 + C_e \quad (4.13)$$

$$A_e = 2\text{Re}[S_e^l S_e^h] c_{23} s_{23}; \quad (4.14)$$

$$B_e = 2\text{Im}[S_e^l S_e^h] c_{23} s_{23}; \quad (4.15)$$

$$C_e = \mathcal{J}_e^l c_{23}^2 + \mathcal{J}_e^h s_{23}^2; \quad (4.16)$$

$$P(\nu_e \rightarrow \nu_\mu) = A_e \cos^2 + B_e \sin^2 + C_e \quad (4.17)$$

$$A_e = 2\text{Re}[S_e^l S_e^h] c_{23} s_{23}; \quad (4.18)$$

$$B_e = 2\text{Im}[S_e^l S_e^h] c_{23} s_{23}; \quad (4.19)$$

$$C_e = \mathcal{J}_e^l s_{23}^2 + \mathcal{J}_e^h c_{23}^2; \quad (4.20)$$

Eqs. (4.13)–(4.16) are the same as those derived in our previous paper [42]. Next, let us derive the approximate formulas for $P(\nu_e \rightarrow \nu_e)$. Using (3.34) directly, we obtain

$$P(\nu_e \rightarrow \nu_e) = C_{ee} = \mathcal{J}_{ee}^0 \quad (4.21)$$

$$= \mathcal{J}_{ee}^l + S_{ee}^h \mathcal{S}_{ee}^d; \quad (4.22)$$

On the other hand, we obtain

$$P(\nu_e \rightarrow \nu_e) = C_{ee} = 1 - C_e - C_\mu \quad (4.23)$$

$$= 1 - \mathcal{J}_e^l - \mathcal{J}_e^h; \quad (4.24)$$

by using the unitarity relation. This is a different approximate formula from (4.22). Thus, there are two kinds of expressions (4.22) and (4.24) for $P(\nu_e \rightarrow \nu_e)$. We can check numerically that the expression (4.24) has a better precision than the expression (4.22). Furthermore the expression (4.24) easily reproduces the approximate formula derived with double expansion up to the second order of two small parameters in ref. [30] (second order formula). So we use the expression (4.24) in the following.

Next, let us derive the approximate formula for $P(\nu_e \rightarrow \nu_\mu)$. At first we calculate the terms independent of the CP phase in this calculation. We can approximate

$$C = \mathcal{J}^0 s_{23}^4 + \mathcal{J}^0 c_{23}^4 + \mathcal{J}^0 (S^0)^2 c_{23}^2 s_{23}^2 + \mathcal{J}^l S^h c_{23}^2 s_{23}^2 \quad (4.25)$$

from (A.47) and (3.35)–(3.36), where we ignore the terms proportional to $\mathcal{J}^0 \mathcal{J}^h = O(\theta_{13}^2)$. This leads to the approximated probability as

$$P(\nu_e \rightarrow \nu_\mu) = B \sin^2 + C \quad (4.26)$$

$$B = 2\text{Im}[S_e^l S_e^h] c_{23} s_{23}; \quad (4.27)$$

$$C = \mathcal{J}^l S^h c_{23}^2 s_{23}^2; \quad (4.28)$$

Next, let us derive the approximate formulas for $P(\nu_e \rightarrow \nu_\tau)$ and $P(\nu_\mu \rightarrow \nu_\tau)$. From (A.35) and (3.35)–(3.36), we obtain

$$C = \mathcal{J}^0 c_{23}^2 + S^0 s_{23}^2 \mathcal{J}^h + (\mathcal{J}^0 \mathcal{J}^l + \mathcal{J}^0 \mathcal{J}^h) c_{23}^2 s_{23}^2 \quad (4.29)$$

$$= \mathcal{J}^l c_{23}^2 + S^h s_{23}^2 \mathcal{J}^h; \quad (4.30)$$

where we neglect the terms proportional to $\mathcal{J}^0 \mathcal{J}^h = O(\theta_{13}^2)$. On the other hand, we obtain another expression by using the unitarity relation as

$$C = 1 - C_e - C_\mu \quad (4.31)$$

$$= 1 - \mathcal{J}_e^l c_{23}^2 - \mathcal{J}_e^h s_{23}^2 - \mathcal{J}^l S^h c_{23}^2 s_{23}^2 \quad (4.32)$$

This seems to be different from (4.30) at a glance. But, we can show that (4.30) and (4.32) are the same expression by using the unitarity relation. In the following, we use the expression (4.32) for the reason that

this easily reproduces the second order formula and we can check the unitarity. In the same way, C is given by

$$C = 1 - C_e - C' = 1 - \mathcal{P}'_e \int s_{23}^2 - \mathcal{P}^h_e \int \mathcal{C}_{23}^2 - \mathcal{P}'^h \int s_{23}^2 \mathcal{C}_{23}^2 \quad (4.33)$$

from the unitarity relation. From the result obtained in sec. 4.1, the approximate formulas for $P(\nu_e \rightarrow \nu_e)$ and $P(\nu_e \rightarrow \nu_\mu)$ are given by

$$P(\nu_e \rightarrow \nu_e) = A \cos + C \quad (4.34)$$

$$A = 2 \text{Re}[\mathcal{P}'_e S^h_e] \mathcal{C}_{23} s_{23}; \quad (4.35)$$

$$C = 1 - \mathcal{P}'_e \int \mathcal{C}_{23}^2 - \mathcal{P}^h_e \int s_{23}^2 - \mathcal{P}'^h \int s_{23}^2 \mathcal{C}_{23}^2 \quad (4.36)$$

$$P(\nu_e \rightarrow \nu_\mu) = A \cos + C \quad (4.37)$$

$$A = 2 \text{Re}[\mathcal{P}'_e S^h_e] \mathcal{C}_{23} s_{23}; \quad (4.38)$$

$$C = 1 - \mathcal{P}'_e \int s_{23}^2 - \mathcal{P}^h_e \int \mathcal{C}_{23}^2 - \mathcal{P}'^h \int \mathcal{C}_{23}^2 s_{23}^2; \quad (4.39)$$

These results are one of the main results of this paper. In all channels, we can present the probabilities including the CP violation by using the amplitudes calculated in two generations. It is noted that the CP violating terms due to the existence of three generations can be calculated from the two generation amplitudes.

Next, let us compare the approximate formulas (4.13)–(4.20), (4.24), (4.26)–(4.28) and (4.34)–(4.39) with the numerical calculations. We take the PREM (Preliminary Reference Earth Model) as the earth matter density profile and compare the approximated values of all probabilities with those calculated numerically. We use the same parameters as those used in fig. 1 and $\sin 2\theta_{23} = 1$, $\theta = 90^\circ$. We set the baseline length, $L = 6000$ km and the energy region, $1 \text{ GeV} \leq E \leq 20 \text{ GeV}$, to include the high energy MSW resonance.

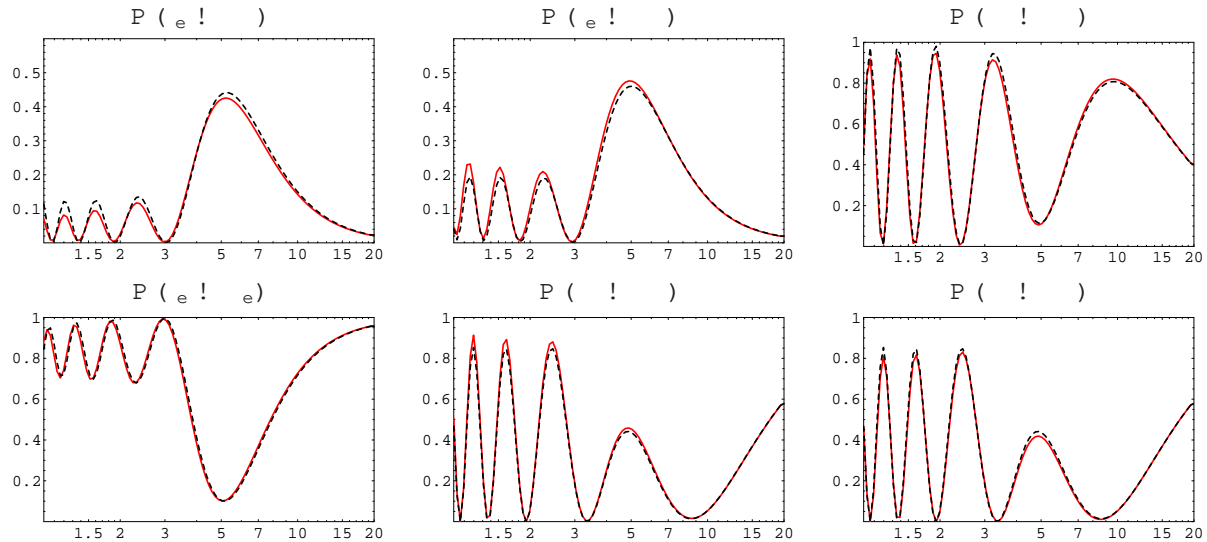


Figure 3: Comparison of our approximate formulas with the numerical calculation. In these figures, it is plotted $P(\nu_e \rightarrow \nu_e)$ to compare our approximate formulas with the numerical calculation. The solid lines show the approximate probabilities and the dashed lines show the numerical calculation of probabilities.

We compare our approximate formulas with the numerical calculation in figure 3. One can see some features from this figure. The approximated value of probabilities for $P(\nu_e \rightarrow \nu_e)$; $P(\nu_e \rightarrow \nu_\mu)$ and $P(\nu_e \rightarrow \nu_\tau)$ coincide to the numerical values very well, on the other hand, the remained three channels of probabilities $P(\nu_\mu \rightarrow \nu_e)$; $P(\nu_\mu \rightarrow \nu_\mu)$ and $P(\nu_\mu \rightarrow \nu_\tau)$ have a little difference between the approximate and the numerical value. However, the difference becomes small compared with figure 2 and we obtain the sufficient result as a first step.

5 Comparison of Our Results with Second Order Formulas

In this section, we concretely calculate the amplitudes by using the approximate formulas derived in the previous section in the case of constant matter. Then, we show that simple approximate formulas can be obtained. Finally, we demonstrate that the approximate formula derived with double expansion up to the second order of two small parameters (second order formulas) are largely different from the exact values in the MSW resonance region under the condition that the baseline length is longer than the oscillation length.

5.1 Approximate Formulas for Amplitudes

In the previous section, we have given a method for approximation of the probabilities in three generations by the amplitudes in two generations. In this subsection, we use the constant matter density profile in order to compare our method with other method and investigate the non-perturbative effects. As seen from (4.13)–(4.20), (4.24), (4.26)–(4.28) and (4.34)–(4.39), we only have to calculate four kinds of amplitudes, namely $S_e^l; S_\mu^l; S_e^h$ and S^h .

The low-energy approximate formulas are obtained by taking the limit $s_{13} = 0$ and we have

$$H^l = O_{12} \text{diag}(0; \theta_{21}; \theta_{31}) O_{12}^T + \text{diag}(a; 0; 0) \quad (5.1)$$

$$= O_{12}^l \text{diag}(\theta_{12}^l; \theta_{21}^l; \theta_{31}^l) (O_{12}^l)^T : \quad (5.2)$$

The effective masses m_i^l ($i = 1; 2$) and the effective mixing angle θ_{12}^l are determined by the diagonalization of (5.1) to (5.2). If we define the mass squared difference in matter as $\Delta_{21}^l = m_2^l{}^2 - m_1^l{}^2$, we obtain the relation

$$\frac{\theta_{21}^l}{\theta_{12}^l} = \frac{\sin 2\theta_{12}^l}{\sin 2\theta_{21}^l} = \frac{s}{\cos 2\theta_{12}^l - \frac{a}{2\Delta_{21}^l} + \sin^2 2\theta_{12}^l} : \quad (5.3)$$

Therefore, the amplitude is calculated as

$$S_e^l = i \sin 2\theta_{12}^l \sin \frac{\theta_{21}^l L}{2} \exp \left[i \frac{\theta_{21}^l + a}{2} L \right] \quad (5.4)$$

$$S_\mu^l = \cos \frac{\theta_{21}^l L}{2} - i \cos 2\theta_{12}^l \sin \frac{\theta_{21}^l L}{2} \exp \left[i \frac{\theta_{21}^l + a}{2} L \right] \quad (5.5)$$

by substituting (5.2) into (3.27). On the other hand, the approximate formulas in high energy are obtained by taking the limit $\theta_{13} = 0$ and we have

$$H^h = O_{13} \text{diag}(0; 0; \theta_{31}) O_{13}^T + \text{diag}(a; 0; 0) \quad (5.6)$$

$$= O_{13}^h \text{diag}(\theta_{13}^h; 0; \theta_{31}^h) (O_{13}^h)^T : \quad (5.7)$$

The effective masses m_i^h ($i = 1; 3$) and the effective mixing angle θ_{13}^h are determined by the diagonalization of (5.6) to (5.7). If we define the mass squared difference in matter as $\Delta_{31}^h = m_3^h{}^2 - m_1^h{}^2$, we obtain the relation

$$\frac{\theta_{31}^h}{\theta_{13}^h} = \frac{\sin 2\theta_{13}^h}{\sin 2\theta_{31}^h} = \frac{s}{\cos 2\theta_{13}^h - \frac{a}{3\Delta_{31}^h} + \sin^2 2\theta_{13}^h} : \quad (5.8)$$

Accordingly, the amplitude can be calculated by substituting (5.7) into (3.28) as

$$S_e^h = i \sin 2\theta_{13}^h \sin \frac{\theta_{31}^h L}{2} \exp \left[i \frac{\theta_{31}^h + a}{2} L \right] \quad (5.9)$$

$$S_\mu^h = \cos \frac{\theta_{31}^h L}{2} - i \cos 2\theta_{13}^h \sin \frac{\theta_{31}^h L}{2} \exp \left[i \frac{\theta_{31}^h + a}{2} L \right] : \quad (5.10)$$

As seen from (5.4) and (5.9), S_e^l and S_e^h have simple forms, but the expressions of S_μ^l and S_μ^h are a little bit complex as (5.5) and (5.10).

5.2 Approximate Formulas for Probabilities

In this subsection, we derive the approximate formulas of the oscillation probabilities in constant matter by using the result of the previous section.

At first, let us consider the case of including electron neutrino in the initial or final state. In this case, the probability for any channel can be calculated almost in the same way. The probability $P(\nu_e \rightarrow \nu_e)$ is obtained by substituting (5.4) and (5.9) into (4.24) as

$$P(\nu_e \rightarrow \nu_e) = 1 - \sin^2 2\theta_{12} \sin^2 \frac{\Delta_{21} L}{2} - \sin^2 2\theta_{13} \sin^2 \frac{\Delta_{31} L}{2} : \quad (5.11)$$

The probability $P(\nu_e \rightarrow \nu_\mu)$ is obtained by substituting (5.4) and (5.9) into (4.14)–(4.16) as

$$P(\nu_e \rightarrow \nu_\mu) = A_e \cos^2 \theta_{13} + B_e \sin^2 \theta_{13} + C_e \quad (5.12)$$

$$A_e = \sin^2 2\theta_{12} \sin^2 2\theta_{23} \sin^2 2\theta_{13} \sin^2 \frac{\Delta_{21} L}{2} \sin^2 \frac{\Delta_{31} L}{2} \cos^2 \frac{\Delta_{32} L}{2} \quad (5.13)$$

$$B_e = \sin^2 2\theta_{12} \sin^2 2\theta_{23} \sin^2 2\theta_{13} \sin^2 \frac{\Delta_{21} L}{2} \sin^2 \frac{\Delta_{31} L}{2} \sin^2 \frac{\Delta_{32} L}{2} \quad (5.14)$$

$$C_e = c_{23}^2 \sin^2 2\theta_{12} \sin^2 \frac{\Delta_{21} L}{2} + s_{23}^2 \sin^2 2\theta_{13} \sin^2 \frac{\Delta_{31} L}{2} : \quad (5.15)$$

The remained probability $P(\nu_e \rightarrow \nu_\tau)$ can be calculated by the unitarity relation. Next, let us calculate the probabilities in the case not including electron neutrino in the initial and final state. Also in this case, the probability for any channel can be calculated almost in the same way. Accordingly, as an example, we take the probability for muon neutrino to tau neutrino,

$$P(\nu_\mu \rightarrow \nu_\tau) = B \sin^2 \theta_{13} + C \quad (5.16)$$

$$B = \sin^2 2\theta_{12} \sin^2 2\theta_{23} \sin^2 2\theta_{13} \sin^2 \frac{\Delta_{21} L}{2} \sin^2 \frac{\Delta_{31} L}{2} \sin^2 \frac{\Delta_{32} L}{2} \quad (5.17)$$

$$C = \sin^2 \theta_{13} \left[s_{23}^2 c_{23}^2 \right] : \quad (5.18)$$

At first, we use the relations, $\cos^2 2\theta_{12} = 2 \cos^2 \theta_{12} - 1$ and $\cos^2 2\theta_{13} = 1 - 2 \sin^2 \theta_{13}$, and we rewrite S^{ν} and S^h as

$$S^{\nu} = \exp \left[-i \frac{\Delta_{21} L}{2} \right] \left[2i \cos^2 \theta_{12} \sin^2 \frac{\Delta_{21} L}{2} \exp \left[-i \frac{\Delta_{21} + a}{2} L \right] \right] \quad (5.19)$$

$$S^h = \exp \left[-i \frac{\Delta_{31} L}{2} \right] + 2i \sin^2 \theta_{13} \sin^2 \frac{\Delta_{31} L}{2} \exp \left[-i \frac{\Delta_{31} + a}{2} L \right] : \quad (5.20)$$

Then, arranging C on the order of the effective mixing angles $\cos^2 \theta_{12}$ and $\sin^2 \theta_{13}$, we obtain

$$C^1 = \sin^2 2\theta_{23} \sin^2 \frac{(\Delta_{21} + \Delta_{31} + \Delta_{32})L}{4} \quad (5.21)$$

$$C^2 = 2 \sin^2 2\theta_{23} \cos^2 \theta_{12} \sin^2 \frac{(\Delta_{21} + \Delta_{31} + \Delta_{32})L}{4} \cos^2 \frac{(\Delta_{21} + \Delta_{31} + \Delta_{32})L}{4} \sin^2 \frac{\Delta_{21} L}{2} \\ + 2 \sin^2 2\theta_{23} \sin^2 \theta_{13} \sin^2 \frac{(\Delta_{21} + \Delta_{31} + \Delta_{32})L}{4} \cos^2 \frac{(\Delta_{21} + \Delta_{31} + \Delta_{32})L}{4} \sin^2 \frac{\Delta_{31} L}{2} \quad (5.22)$$

$$C^3 = \sin^2 2\theta_{23} \cos^4 \theta_{12} \sin^2 \frac{\Delta_{21} L}{2} + \sin^2 2\theta_{23} \sin^4 \theta_{13} \sin^2 \frac{\Delta_{31} L}{2} \\ + 2 \sin^2 2\theta_{23} \cos^2 \theta_{12} \sin^2 \theta_{13} \sin^2 \frac{\Delta_{21} L}{2} \sin^2 \frac{\Delta_{31} L}{2} \cos^2 \frac{\Delta_{32} L}{2} : \quad (5.23)$$

As we show in the following section, the reason of arranging like this is because the second order formulas are easily derived from this form. In order to derive the second order formulas, it is sufficient to use C^1 and C^2 . We can also calculate the other channels $P(\nu_\mu \rightarrow \nu_e)$ and $P(\nu_\tau \rightarrow \nu_e)$ in the same way. In recent study, it is found that the channels $P(\nu_\mu \rightarrow \nu_e)$ and $P(\nu_\tau \rightarrow \nu_e)$ are largely affected by the earth matter in the long baseline [45, 46, 47].

We can see from these expressions that the approximate formulas are a little bit complex in the case for not including electron neutrino in the initial or final state. We also understand from these formulas how the matter affect the probabilities. Furthermore, there is another advantage for studying the magnitude of the CP violation. Thus, the formulas are expected to be useful in the case that we consider the matter effects.

5.3 Large N non-perturbative Effects of small θ_{13} and s_{13}

In this subsection, we compare the approximate formulas obtained in the previous subsection with the second order formulas numerically and it is shown that the latter have a large difference from the numerical value in the MSW resonance region.

The second order formulas are approximated by the main terms of the expansion and are widely used by many authors for their simplicity. In refs. [28, 29], the formula for $P(\nu_e \rightarrow \nu_e)$ has been derived and after that all probabilities have been given in ref. [30]. As examples, the probabilities, $P(\nu_e \rightarrow \nu_e)$ and $P(\nu_e \rightarrow \nu_\mu)$, are taken. For the other channels of the probabilities, similar expressions have been obtained. In all channels the similar result are obtained from the comparison with the numerical calculation. The second order formula for $P(\nu_e \rightarrow \nu_e)$ is given by

$$P(\nu_e \rightarrow \nu_e) = A_e \cos^2 + B_e \sin^2 + C_e ; \quad (5.24)$$

$$A_e \approx s_{13} \sin^2 2\theta_{12} \sin^2 2\theta_{23} \frac{2 \sin^2 \theta_{31}}{a(\sin \theta_{31} - a)} \sin^2 \frac{aL}{2} \sin^2 \frac{(\sin \theta_{31} - a)L}{2} \cos^2 \frac{32L}{2} \quad (5.25)$$

$$B_e \approx s_{13} \sin^2 2\theta_{12} \sin^2 2\theta_{23} \frac{2 \sin^2 \theta_{31}}{a(\sin \theta_{31} - a)} \sin^2 \frac{aL}{2} \sin^2 \frac{(\sin \theta_{31} - a)L}{2} \sin^2 \frac{32L}{2} \quad (5.26)$$

$$C_e \approx C_{23}^2 \sin^2 2\theta_{12} \frac{\sin^2 \theta_{31}}{a^2} \sin^2 \frac{aL}{2} + s_{13}^2 s_{23}^2 \frac{4 \sin^2 \theta_{31}}{(\sin \theta_{31} - a)^2} \sin^2 \frac{(\sin \theta_{31} - a)L}{2} ; \quad (5.27)$$

Comparing our approximate formulas (5.13)–(5.15) with the second order formulas (5.25)–(5.27), each term corresponds one to one. Actually, the second order formulas (5.25)–(5.27) are derived by expanding our approximate formulas (5.13)–(5.15) up to the second order in θ_{13} and s_{13} [42]. Next, the second order formula for $P(\nu_e \rightarrow \nu_\mu)$ is given by

$$P(\nu_e \rightarrow \nu_\mu) = A \cos^2 + B \sin^2 + C \quad (5.28)$$

$$A \approx s_{13} \sin^2 2\theta_{23} \sin^2 2\theta_{12} \cos^2 2\theta_{31} \frac{2 \sin \theta_{31}}{a} \sin^2 \frac{31L}{2} - \frac{a}{\sin \theta_{31}} \sin^2 \frac{31L}{2} - \frac{\sin \theta_{31}}{a} \sin^2 \frac{aL}{2} \cos^2 \frac{(\sin \theta_{31} - a)L}{2} \quad (5.29)$$

$$B \approx s_{13} \sin^2 2\theta_{12} \sin^2 2\theta_{23} \frac{2 \sin^2 \theta_{31}}{a(\sin \theta_{31} - a)} \sin^2 \frac{aL}{2} \sin^2 \frac{(\sin \theta_{31} - a)L}{2} \sin^2 \frac{32L}{2} ; \quad (5.30)$$

and C is given by

$$C \approx \sin^2 2\theta_{23} \sin^2 \frac{31L}{2} - \sin^2 2\theta_{23} \cos^2 2\theta_{12} \frac{\sin \theta_{31}}{2} \sin^2 31L + \sin^2 2\theta_{23} \cos^4 2\theta_{12} \frac{\sin^2 \theta_{31}}{2} \cos^2 31L - 2 \sin^2 2\theta_{23} \sin^2 2\theta_{12} \frac{\sin \theta_{31}}{2a} \sin^2 \frac{31L}{2} \cos^2 \frac{(\sin \theta_{31} - a)L}{2} \sin^2 \frac{aL}{2} - \frac{\sin \theta_{31}}{a} \sin^2 \frac{31L}{4} - \frac{2 \sin^2 \theta_{31}}{31} \sin^2 2\theta_{23} \frac{2 \sin \theta_{31}}{a} \sin^2 \frac{31L}{2} \cos^2 \frac{aL}{2} \sin^2 \frac{(\sin \theta_{31} - a)L}{2} - \frac{\sin \theta_{31}}{31} \frac{aL}{a} \sin^2 \frac{31L}{4} ; \quad (5.31)$$

Thus, the second order formula for C is rather complex. Comparing our approximate formula (5.21)–(5.23) with the second order formula (5.31), A is not included in our formula. The reason is that $A = 0$ in the case of the maximal mixing angle $\sin 2\theta_{23} = 1$ and we cannot calculate this from the method described in this paper. If we consider $\cos 2\theta_{23}$ as a small parameter like θ_{13} and s_{13} , this A has the magnitude of $O(s_{13} \cos 2\theta_{23})$. Therefore, A is proportional to the third order of small parameters and is expected to be very small. This means that our formula is not largely affected by the error due to this term, which cannot be derived from our method. However, as this error affects to the precision measurement of $\sin 2\theta_{23}$ by the atmospheric neutrino experiments in future, the improvement of this point is the future work. The formulas for the other channels are given in ref. [30]. The second order formulas are effective under the following two conditions.

The first one is for the neutrino energy and is given by

$$E \approx 0.45 \text{ GeV} \frac{m_{21}^2}{10^4 \text{ eV}^2} \frac{3g = \text{cm}^3}{\text{cm}^3} ; \quad (5.32)$$

The second one is for the baseline length and is given by

$$L = 8000 \text{ km} \frac{E}{\text{GeV}} \frac{10^4 \text{ eV}^2}{m_{21}^2} : \tag{5.33}$$

These conditions come from the utilization of perturbative expansion on two small parameters. The detailed discussion are given in [29]. These formulas are used by many authors for their simplicity [48, 49]. However, as shown in the next figure, there is a problem for these formulas to have large difference from the true value in the MSW resonance region, which is considered to be most important region.

Next, let us compare our formulas (5.12)–(5.22) with the second order formulas (5.24)–(5.31) in all channels by numerical calculation. In order to see the magnitude of the error, we also compare two kinds of approximate formulas with the exact values. We set the baseline length as $L = 6000 \text{ km}$, where the MSW effect becomes large, and the energy region as $1 \text{ GeV} \leq E \leq 20 \text{ GeV}$, where the MSW resonance energy is included. Furthermore, the second order formulas are derived only in the case of constant matter, so we choose the average density $\rho = 3.91 \text{ g/cm}^3$ of the earth calculated by the PREM. Note that two conditions (5.32) and (5.33) are satisfied in these region.

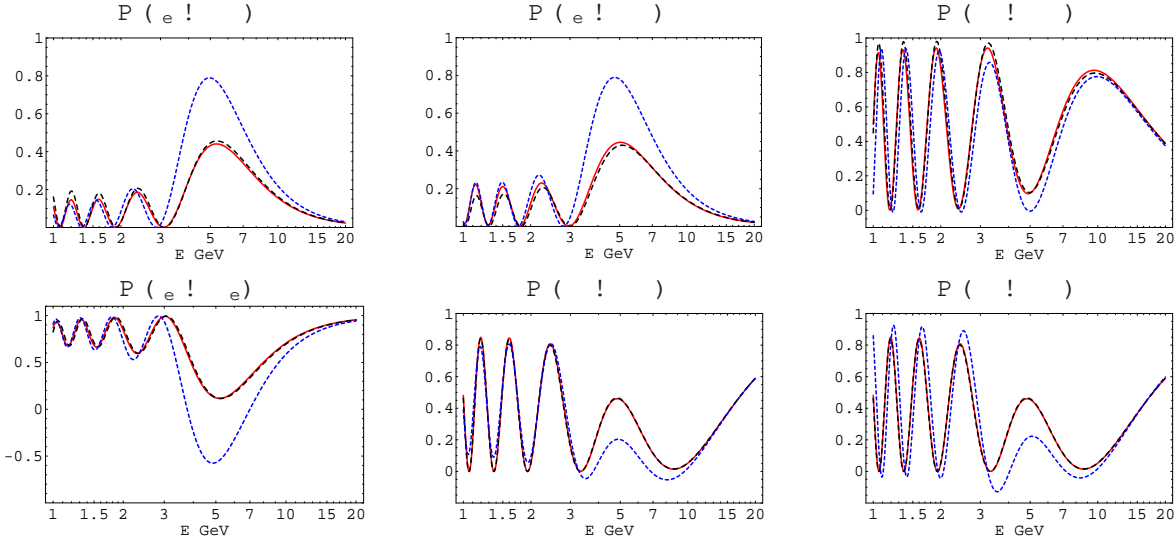


Figure 4: Comparison of our approximate formulas with the second order formulas. These figures are plotted to compare our approximate formulas with the second order formulas and in addition to the numerical calculation. The solid, dashed and dotted lines show the probabilities in our approximate formulas, those in the numerical calculation and those in the second order formulas, respectively.

We compare the probabilities calculated by our approximate formulas in all channels with those by the second order formulas in addition to numerical calculation in figure 4. One can see the following points from this figure. The second order formulas have large difference from the numerical values around 5 GeV, while these are good coincidence in other energy region. This means that the second order formulas are broken out around 5 GeV, where the high energy MSW resonance occurs. The value of $P(\nu_e \rightarrow \nu_e)$ has the largest difference. The probabilities $P(\nu_e \rightarrow \nu_\mu)$ and $P(\nu_e \rightarrow \nu_\tau)$ have the next largest difference. The values of $P(\nu_\mu \rightarrow \nu_\mu)$ and $P(\nu_\tau \rightarrow \nu_\tau)$ have relatively large difference. The smallest difference is realized in the probability $P(\nu_\mu \rightarrow \nu_\tau)$. In addition, these figures show that the difference between the second order formulas and the numerical calculation exists even in the two applicable regions (5.32) and (5.33). Although we do not show figure, the difference between our approximate formulas (5.12)–(5.22) and the second order formulas (5.24)–(5.31) become more clear out of the two applicable regions (5.32) and (5.33). The reason is that our approximate formulas (5.12)–(5.22) are applicable even for the case that the condition (5.32) or (5.33) for energy and baseline length does not hold, as confirmed from the comparison with the exact numerical calculation. However, the second order formulas have a good coincidence if the neutrino energy is not on the resonance energy even for the long baseline length.

6 Non-perturbative Effects of Small Parameters $m_{21}^2 = m_{31}^2$ and $\sin \theta_{13}$

In this section, we investigate the reason for the difference between second order formulas (the approximate formula derived with double expansion up to the second order of two small parameters) and the numerical calculation around the MSW resonance region as confirmed in the previous subsection. We give a discussion about non-perturbative effects of small mixing angle more detail than that in section 2.

6.1 Derivation of the Second Order Formulas

In this subsection, we investigate how the second order formulas are approximated expanding on $\theta_{13} = \theta_{13}^h$, $m_{21}^2 = m_{31}^2$. In the previous paper, we have discussed the probability $P(\nu_e \rightarrow \nu_\mu)$, so we calculate the second order formula for $P(\nu_e \rightarrow \nu_\tau)$ here. The method of calculation is basically the same but the calculation itself become complex a little because we need to calculate the effective mass and the effective mixing angle up to the second order of θ_{13} and s_{13} in the case of $P(\nu_e \rightarrow \nu_\tau)$. In this point, the calculation is not straightforward compared with that of $P(\nu_e \rightarrow \nu_\mu)$ but the method of approximation is the same. At first, we describe C up to the second order of $\cos \theta_{12}^h$ and $\sin \theta_{13}^h$ as

$$C^1 = \sin^2 2\theta_{23} \sin^2 \frac{(\theta_{21}^h + \theta_{31}^h + \theta_{32})L}{4} \quad (6.1)$$

$$C^{2a} = 2 \sin^2 2\theta_{23} \cos^2 \theta_{12}^h \sin \frac{(\theta_{21}^h + \theta_{31}^h + \theta_{32})L}{4} \cos \frac{(\theta_{21}^h - \theta_{31}^h - \theta_{32})L}{4} \sin \frac{\theta_{21}^h L}{2} \quad (6.2)$$

$$C^{2b} = 2 \sin^2 2\theta_{23} \sin^2 \theta_{13}^h \sin \frac{(\theta_{21}^h + \theta_{31}^h + \theta_{32})L}{4} \cos \frac{(\theta_{21}^h - \theta_{31}^h + \theta_{32})L}{4} \sin \frac{\theta_{31}^h L}{2}; \quad (6.3)$$

where we separate for $C^2 = C^{2a} + C^{2b}$, as the simplicity of the discussion given later. Note that C^1 does not include the effective mixing angle. For this reason, although we need to expand the effective mass up to the second order to calculate the probability up to the second order in θ_{13} and s_{13} , it is enough to expand the effective mixing angle up to the zeroth order. The effective mixing angle is expanded up to the zeroth order as

$$\cos \theta_{12}^h \approx \frac{1}{2} \sin 2\theta_{12}^h \approx \sin 2\theta_{12} \frac{31}{2a} \quad (6.4)$$

$$\sin \theta_{13}^h \approx \frac{1}{2} \sin 2\theta_{13}^h \approx s_{13} \frac{31}{31a} \quad (6.5)$$

and the effective mass is expanded up to the second order as

$$\theta_{21}^h \approx a \cos 2\theta_{12} \frac{31}{31} + \frac{1}{2} \sin^2 2\theta_{12} \frac{31^2}{2a} \quad (6.6)$$

$$\theta_{31}^h \approx \theta_{31} + \frac{1}{2} \frac{2\theta_{31}a}{31a}; \quad (6.7)$$

Here, it is noted the following points. Eqs. (6.4) and (6.6) obtained by the expansion in θ_{13} diverge in the vacuum limit $a \rightarrow 0$ and eqs. (6.5) and (6.7) obtained by the expansion in s_{13} diverge in the high energy MSW resonance limit $a \rightarrow 31$. As shown in the following, these divergences cancel and the probability has a finite value. Expanding C^1 up to the second order, we obtain

$$C^1 \approx C^{1a} + C^{1b} + C^{1c} + C^{1d} + C^{1e} \quad (6.8)$$

$$C^{1a} = \sin^2 2\theta_{23} \sin^2 \frac{31L}{2} \quad (6.9)$$

$$C^{1b} = \sin^2 2\theta_{23} \cos^2 \theta_{12} \frac{31L}{2} \sin \theta_{31}L \quad (6.10)$$

$$C^{1c} = 2 \sin^2 2\theta_{23} \cos^4 \theta_{12} \frac{31L}{2} \cos^2 \theta_{31}L \quad (6.11)$$

$$C^{1d} = 2 \sin^2 2\theta_{23} \sin^2 2\theta_{12} \frac{31L}{8a} \sin \theta_{31}L \quad (6.12)$$

$$C^{1e} = s_{13}^2 \sin^2 2\theta_{23} \frac{a}{31} \frac{31L}{2a} \sin \theta_{31}L; \quad (6.13)$$

We also expand C^{2a} and C^{2b} as

$$C^{2a} = \sin^2 \theta_{23} \sin^2 \theta_{12} \frac{s_{31}^2}{2a} \sin^2 \frac{31L}{2} \cos \left(\frac{31-a}{2} L \right) \sin \frac{aL}{2} \quad (6.14)$$

$$C^{2b} = s_{13}^2 \sin^2 \theta_{23} \frac{s_{31}^2}{a} \sin^2 \frac{31L}{2} \cos \frac{aL}{2} \sin \left(\frac{31-a}{2} L \right); \quad (6.15)$$

Finally, we obtain (5.31) arranging these result order by order.

Here, let us consider the applicable region of the second order formulas. C^{1d} diverges in the limit $a \rightarrow 0$ and C^{1e} diverges in the limit $a \rightarrow s_{31}$. C^{2a} also diverges in the limit $a \rightarrow 0$ and C^{2b} diverges in the limit $a \rightarrow s_{31}$. The divergences in $a \rightarrow 0$ and in $a \rightarrow s_{31}$ come from the expansion of the effective masses (6.6) and (6.7) respectively.

It seems that the second order formulas do not reduce to those in vacuum due to the divergence in $a \rightarrow 0$ and furthermore do not reduce to those in the high energy MSW resonance point due to the divergence in $a \rightarrow s_{31}$. However, when we consider the pair

$$C^{1d} + C^{2a} = \sin^2 \theta_{23} \sin^2 \theta_{12} \frac{s_{31}}{2a} \sin \frac{31L}{2} \cos \left(\frac{31-a}{2} L \right) \sin \frac{aL}{2} - \frac{s_{31}}{a} - \frac{s_{31}L}{4} \sin(s_{31}L) \quad (6.16)$$

the divergence in $a \rightarrow 0$ cancel and the value converges. The obtained finite value is given by

$$\lim_{a \rightarrow 0} (C^{1d} + C^{2a}) = \sin^2 \theta_{23} \sin^2 \theta_{12} \frac{1}{2} \frac{s_{31}^2}{2} \sin^2 \frac{31L}{2}; \quad (6.17)$$

Before we expand, C^{1d} and C^{2a} have finite values in the limit $a \rightarrow 0$ and $a \rightarrow s_{31}$. However, the divergence appears in expansion of θ_{12} and s_{13} . The cancellation of these divergences occurs between C^{1d} and C^{2a} . This means that the cancellation occurs between the different terms to have the finite values respectively, at first. It is an interesting result. Considering the pair as

$$C^{1e} + C^{2b} = s_{13}^2 \sin^2 \theta_{23} \frac{2s_{31}}{31-a} \sin \frac{31L}{2} \cos \frac{aL}{2} \sin \left(\frac{31-a}{2} L \right) - \frac{s_{31}}{31-a} - \frac{aL}{4} \sin(s_{31}L); \quad (6.18)$$

the divergence in the limit $a \rightarrow s_{31}$ cancels and the value converges. The finite value is given by

$$\lim_{a \rightarrow s_{31}} (C^{1e} + C^{2b}) = s_{13}^2 \sin^2 \theta_{23} \frac{s_{31}L}{2} \sin(s_{31}L) \sin^2 \frac{31L}{2} - \sin(s_{31}L); \quad (6.19)$$

The cancellation of these divergences occurs between the different terms C^{1e} and C^{2b} . This is also interesting.

We have shown that the second order formulas have finite values in the limit $a \rightarrow 0$ and $a \rightarrow s_{31}$, but it is not always the same as that in the numerical calculation. Actually, the difference in Fig. 4 in the limit $a \rightarrow s_{31}$, shows that the second order formulas have finite values but they are not in accordance with those in the numerical calculation. In order to study this, we compare the three quantities, the numerical calculation, our formulas and the second order formulas. We can learn the differences mainly in the vacuum limit $a \rightarrow 0$ and the high energy MSW resonance limit $a \rightarrow s_{31}$ from the comparison.

At first, let us consider the vacuum limit $a \rightarrow 0$. Furthermore, to simplify the discussion, we consider the case of $s_{13} \rightarrow 0$. The second order formulas in the limits $a \rightarrow 0$ and $s_{13} \rightarrow 0$ are given by

$$\begin{aligned} \lim_{a; s_{13} \rightarrow 0} C^{(\text{double})} &= \sin^2 \theta_{23} \sin^2 \frac{31L}{2} - \sin^2 \theta_{23} \cos^2 \theta_{12} \frac{s_{31}L}{2} \sin s_{31}L \\ &+ \sin^2 \theta_{23} \cos^4 \theta_{12} \frac{s_{31}L}{2} \cos s_{31}L \\ &- \sin^2 \theta_{23} \sin^2 \theta_{12} \frac{1}{2} \frac{s_{31}L}{2} \sin^2 \frac{31L}{2}; \end{aligned} \quad (6.20)$$

Next, taking the limit $a \rightarrow 0$ and $s_{13} \rightarrow 0$ in our formulas, we obtain

$$\begin{aligned} \lim_{a; s_{13} \rightarrow 0} C^{(\text{exact})} &= \sin^2 \theta_{23} \sin^2 \frac{31L}{2} \\ &- 2 \sin^2 \theta_{23} \cos^2 \theta_{12} \sin \frac{31L}{2} \cos \left(\frac{21-31}{2} L \right) \sin \frac{21L}{2}; \end{aligned} \quad (6.21)$$

Expanding the oscillating part of (6.21) in our formula, it leads to (6.20) obtained from the second order formula. The condition for the expansion on the oscillating part to be a good approximation is

$$L < \frac{2}{21} : \quad (6.22)$$

Next, let us consider the high energy M SW resonance limit $a \rightarrow \infty$. Furthermore, to simplify the discussion, we take the high energy M SW resonance limit $a \rightarrow \infty$ under the condition $\theta \neq 0$. In the high energy M SW resonance limit of the second order formula, we obtain

$$\begin{aligned} \lim_{a \rightarrow \infty} C^{(\text{double})} &= \sin^2 2\theta_{23} \sin^2 \frac{31L}{2} \\ &+ s_{13}^2 \sin^2 2\theta_{23} \frac{31L}{2} (\sin 31L) \sin^2 \frac{31L}{2} \sin(31L) : \quad (6.23) \end{aligned}$$

Next, taking the limit $a \rightarrow \infty$ and $\theta \neq 0$ in our formulas, we obtain

$$\begin{aligned} \lim_{a \rightarrow \infty} C^{(\text{exact})} &= \sin^2 2\theta_{23} \sin^2 \frac{(1 + s_{13}) 31L}{2} \\ &\sin^2 2\theta_{23} (1 - s_{13}^2) \sin \frac{(1 + s_{13}) 31L}{2} \cos \frac{(1 - s_{13}) 31L}{4} \sin(s_{13} 31L) : \quad (6.24) \end{aligned}$$

Expanding the oscillating part obtained from our formula (6.24), it is shown that this coincides with that from the second order formula (6.23). The condition for the expansion of the oscillating part to be a good approximation is given by

$$L < \frac{2}{s_{13} 31} = \frac{2}{s_{13} a} : \quad (6.25)$$

If the baseline length is shorter than that obtained from above condition, the second order formula becomes a good approximation. We obtain the following results about the perturbative expansion on the small parameters θ and s_{13} .

1. The perturbative expansion in θ actually corresponds to the expansion in $\theta_{21} = a$. This constrains the applicable energy for the approximate formulas. If we expand in the parameter $\theta_{21} = a$, the effective mass m_{21} and the effective mixing angle $\sin 2\theta_{12}$ diverge in the vacuum limit $a \rightarrow 0$. However, these divergences cancel each other in calculating the oscillation probability. Thus, the probability has a finite value, but the value largely differs from the numerical calculation in low-energy. The magnitude of this difference becomes large and serious in the case of small mixing angle and in low-energy long baseline experiments.
2. If we expand in the small mixing angle s_{13} , the effective mass m_{31} and the effective mixing angle $\sin 2\theta_{13}$ diverge in the M SW resonance energy limit $a \rightarrow \infty$. However, these divergences also cancel each other in calculating the oscillation probability. Thus, the probability has a finite value, but the value largely differs from the numerical calculation in the high-energy M SW resonance region. This means that the second order formulas cannot be used in the high energy M SW resonance region.

In two generations, we can calculate the oscillation probabilities exactly by solving the second order equation. So, we do not need the perturbative expansion. On the other hand, the construction of the approximate formulas applicable to arbitrary matter density profile is very difficult in three generations. Therefore, we need to expand on the small parameters θ and s_{13} .

6.2 Discussion

We have shown that the double expansion formulas up to the second order in the two small parameters θ and s_{13} does not give a good approximation in the M SW resonance region. This is because the coefficients of the small parameters have large values in the M SW resonance region. In this subsection, let us discuss some methods proposed up to present to solve this problem. The Hamiltonian H^0 is written by four parameters. Two parameters ($m_{21}^2; \theta_{12}$) control the physics mainly in low-energy and the other two parameters ($m_{31}^2; \theta_{13}$) control the physics mainly in high-energy. In other words, the magnitude of θ determines low-energy phenomena and the magnitude of s_{13} determines high-energy phenomena. Both these parameters are

very small but the energy region where the expansion is convergent is different. This means that we need to treat the applicable energy region carefully when we expand on these two parameters. Based on these facts, let us consider the approximate formulas one more time.

Comparing the perturbative expansion with numerical calculation, we have shown that we need to take into account the higher order terms of θ and s_{13} for deriving the formulas, which give a good approximation even in the MSW resonance points. Because the perturbative expansion on θ breaks down in low-energy region and the expansion on s_{13} also breaks down in high-energy region. There are several methods in order to take into account the higher order terms of θ and s_{13} as follows.

1. exact formulas in constant matter density profile
2. reduction formulas taking into account the two generation part exactly

In the first one, there does not exist the error generated from the perturbative expansion, because of the exact treatment of both θ and s_{13} [40]. Furthermore, non-perturbative effects can be easily investigated by using these exact formulas. The second one is the method introduced in this paper. In this method, we try to include the higher order terms of θ and s_{13} partially, except for the terms including the product of two small parameters. This method takes the higher order terms of θ and s_{13} simply and applicable even in the case of arbitrary matter density profile [42, 43]. Although this method is two generation approximation of the amplitude, it has the notable feature that the three generation effects such as CP violation can be calculated.

The discussion above is summarized as follows. Although the second order formulas have a very simple form, it does not coincide with the numerical calculation around the low and high energy MSW regions. This means that the perturbative expansion breaks down in these regions and we need to consider the non-perturbative effects, namely the higher order terms of s_{13} and θ . Although the second order formulas give good approximations, if it is not MSW resonance point, we need to take into account non-perturbative effects to construct the approximate formulas which coincide with the numerical calculation even in the MSW resonance region.

7 Summary

In this paper, we consider the method which approximates the neutrino oscillation probabilities in matter under three generations. We summarize the results obtained in this paper.

1. In the framework of two generation neutrino oscillation, we discuss the applicable region of the perturbative expansion on the small mixing angle in matter. The result of the perturbation differs largely from the exact numerical calculation in the MSW resonance point. This means that non-perturbative effects are important even for the neutrino oscillation in two generations.
2. We propose a method calculating the approximate formulas in which non-perturbative effects of the small parameters $m_{21}^2 = m_{31}^2$ and $\sin^2 \theta_{13}$. Under the conditions, $\theta_{23} = 45^\circ$ and the symmetric matter density profile, we derive simple approximate formulas of the probabilities in all channels by using the unitarity relation. Although all these approximate formulas are expressed by the amplitudes calculated within the framework of two generations, it has a notable feature that the three generation effects such as CP violation can be calculated.
3. In three generation neutrino oscillation with matter, we investigate non-perturbative effects of the two small parameters $m_{21}^2 = m_{31}^2$ and $\sin^2 \theta_{13}$. We compare our approximate formulas with those from the double expansion which include the terms up to the second order in low and high energy MSW resonance regions. As the result, we have shown that the second order formulas have large differences from the exact numerical calculation. This means that non-perturbative effects of the small $m_{21}^2 = m_{31}^2$ and $\sin^2 \theta_{13}$ become important in the MSW resonance region.

Finally, we describe the two problems that we cannot fully address enough in this paper.

1. The approximate formulas are derived in this paper by using the condition $\theta_{23} = 45^\circ$. Although this condition $\theta_{23} = 45^\circ$ is the center value obtained from the atmospheric neutrino experiments, the difference may exist from this value within 90% confidence level.

2. The condition for the symmetric matter density is satisfied in the 1-dimensional model like the PREM and the ak135f, but the actual matter density, for example, that from J-PARC to Beijing is not symmetric [50]. Therefore, we would like to derive the approximate formulas that hold not only in symmetric matter but in arbitrary matter as well.

To solve the above two problems are the future works.

Acknowledgement

We are grateful to H. Yokoyama and T. Yoshikawa for useful discussions and the careful reading of our manuscript.

A General Feature of CP Dependence

We concretely calculate the coefficients of the probabilities in Appendix A. We show that the 2-3 mixing angle and the CP phase are not affected by matter, from the different point of view described in our previous paper [39]. This result means that we only have to consider the matter effects on four parameters ($m_{21}^2; \theta_{12}$) and ($m_{31}^2; \theta_{13}$). By using this result, we can understand the matter effects in three generations which become complex compared with that in two generations.

A.1 Remarkable Features of Effective Masses

In this subsection, we show that ($\theta_{23}; \delta$) do not affect the effective mass in three generation Hamiltonian. If we express the effective Hamiltonian in matter as

$$H = U \text{diag}(0; m_{21}^2; m_{31}^2) U^\dagger + \text{diag}(a; 0; 0); \quad (\text{A } 1)$$

the equation of eigenvalue is given by

$$\det(t - H) = t^3 - (m_{21}^2 + m_{31}^2 + a)t^2 + (m_{21}^2 m_{31}^2 + a(m_{21}^2(1 - |J_{e2}|^2) + m_{31}^2(1 - |J_{e3}|^2)))t - a m_{21}^2 m_{31}^2 |J_{e1}|^2 = 0; \quad (\text{A } 2)$$

and by solving this equation, we obtain the effective masses as

$$m_1 = \frac{A}{3} - \frac{1}{3} \sqrt{\frac{A^2 - 3BS}{A^2 - 3BS}} \sqrt{\frac{A^2 - 3BS}{A^2 - 3BS} - 1} \sqrt{S^2} \quad (\text{A } 3)$$

$$m_2 = \frac{A}{3} - \frac{1}{3} \sqrt{\frac{A^2 - 3BS}{A^2 - 3BS} + \frac{A^2 - 3BS}{A^2 - 3BS} - 1} \sqrt{S^2} \quad (\text{A } 4)$$

$$m_3 = \frac{A}{3} + \frac{2}{3} \sqrt{\frac{A^2 - 3BS}{A^2 - 3BS}} \quad (\text{A } 5)$$

[44], where $A; B; C$ and S are defined by

$$A = m_{21}^2 + m_{31}^2 + a \quad (\text{A } 6)$$

$$B = m_{21}^2 m_{31}^2 + a[m_{21}^2(1 - |J_{e2}|^2) + m_{31}^2(1 - |J_{e3}|^2)] \quad (\text{A } 7)$$

$$C = a m_{21}^2 m_{31}^2 |J_{e1}|^2 \quad (\text{A } 8)$$

$$S = \cos \frac{1}{3} \arccos \frac{2A^3 - 9AB + 27C}{2(A^2 - 3B)^{3/2}} \quad (\text{A } 9)$$

These effective masses depend only on the following three vacuum mixing angles

$$|J_{e1}| = c_{12}c_{13}; \quad |J_{e2}| = s_{12}c_{13}; \quad |J_{e3}| = s_{13}. \quad (\text{A } 10)$$

One can see from these that the effective masses are independent of the 2-3 mixing angle θ_{23} and the CP phase δ . Next, let us consider this result from a different point of view.

A.2 Decomposition of 2-3 mixing and CP Phase from Hamiltonian

In this section, we separate θ_{23} and δ from the Hamiltonian and we study the dependence of the amplitudes on the two small parameters θ_{12} and s_{13} . The Standard Parametrization is defined by

$$U = O_{23} O_{13} {}^y O_{12}; \quad (\text{A } 11)$$

where the CP phase matrix is given by

$$= \text{diag}(1; 1; e^{i\delta}): \quad (\text{A } 12)$$

The CP phase matrix and the 1-2 mixing matrix O_{12} are commutable as

$$[; O_{12}] = [; \text{diag}(0; \theta_{12}; \theta_{12})] = 0: \quad (\text{A } 13)$$

Therefore, the Hamiltonian can be separated as

$$H(t) = U \text{diag}(0; \theta_{12}; \theta_{12}) U^y + \text{diag}(a(t); 0; 0) = O_{23} H^0(t) {}^y O_{23}^T; \quad (\text{A } 14)$$

where $H^0(t)$ is defined by

$$H^0(t) = O_{13} O_{12} \text{diag}(0; \theta_{12}; \theta_{12}) O_{12}^T O_{13}^T + \text{diag}(a(t); 0; 0): \quad (\text{A } 15)$$

This means that the 2-3 mixing and the CP phase can be separated from the part which includes the matter effects $a(t)$.

In the case of constant matter density profile, we obtain

$$\det(H) = \det(H^0); \quad (\text{A } 16)$$

the 2-3 mixing angle and the CP phase do not affect the eigenvalue equation. Accordingly, the effective masses are independent of the 2-3 mixing angle and the CP phase, which coincide with the result obtained in the previous subsection.

A.3 Exact CP and 2-3 mixing Dependence of Oscillation Probabilities

Here, let us consider the case in which we apply the above discussion used in the Hamiltonian to the amplitude. Solving the Schrodinger eq. for the amplitude in matter, we obtain

$$S(t) = T \exp \int_0^t i H(t) dt : \quad (\text{A } 17)$$

By using this, we obtain

$$S(t) = T \exp \int_0^t i O_{23} H^0(t) {}^y O_{23}^T dt = O_{23} T \exp \int_0^t i H^0(t) dt {}^y O_{23}^T = O_{23} S^0(t) {}^y O_{23}^T \quad (\text{A } 18)$$

from (A.14). Therefore, $S(t)$ satisfies

$$S(t) = O_{23} S^0(t) {}^y O_{23}^T: \quad (\text{A } 19)$$

From this equation, we obtain

$$P(e \rightarrow e) = C_{ee}; \quad (\text{A } 20)$$

$$P(\mu \rightarrow \mu) = A \cos^2 + B \sin^2 + C; \quad (\text{A } 21)$$

when the initial or final state is e , and

$$P(\mu \rightarrow \tau) = A \cos^2 + B \sin^2 + C + D \cos 2\theta + E \sin 2\theta; \quad (\text{A } 22)$$

in the case of $\delta = \delta$; [39]. The final result is given by

$$P(\nu_e \rightarrow \nu_e) = C_{ee} = \mathfrak{P}_{ee}^0 \mathfrak{J}; \quad (\text{A } 23)$$

$$P(\nu_e \rightarrow \nu_\mu) = A_e \cos \delta + B_e \sin \delta + C_e; \quad (\text{A } 24)$$

$$A_e = 2\text{Re}[\mathfrak{S}_e^0 S_e^0] c_{23} s_{23}; \quad (\text{A } 25)$$

$$B_e = 2\text{Im}[\mathfrak{S}_e^0 S_e^0] c_{23} s_{23}; \quad (\text{A } 26)$$

$$C_e = \mathfrak{P}_e^0 \mathfrak{J} c_{23}^2 + \mathfrak{P}_e^0 \mathfrak{J} s_{23}^2; \quad (\text{A } 27)$$

$$P(\nu_e \rightarrow \nu_\tau) = A_e \cos \delta + B_e \sin \delta + C_e; \quad (\text{A } 28)$$

$$A_e = 2\text{Re}[\mathfrak{S}_e^0 S_e^0] c_{23} s_{23}; \quad (\text{A } 29)$$

$$B_e = 2\text{Im}[\mathfrak{S}_e^0 S_e^0] c_{23} s_{23}; \quad (\text{A } 30)$$

$$C_e = \mathfrak{P}_e^0 \mathfrak{J} s_{23}^2 + \mathfrak{P}_e^0 \mathfrak{J} c_{23}^2; \quad (\text{A } 31)$$

$$P(\nu_\mu \rightarrow \nu_\mu) = A \cos \delta + B \sin \delta + C + D \cos 2\delta + E \sin 2\delta; \quad (\text{A } 32)$$

$$A = 2\text{Re}[(S^0 c_{23}^2 + S^0 s_{23}^2) (S^0 + S^0)] c_{23} s_{23}; \quad (\text{A } 33)$$

$$B = 2\text{Im}[(S^0 c_{23}^2 + S^0 s_{23}^2) (S^0 - S^0)] c_{23} s_{23}; \quad (\text{A } 34)$$

$$C = \mathfrak{P}^0 \mathfrak{J} c_{23}^4 + \mathfrak{P}^0 \mathfrak{J} s_{23}^4 + (\mathfrak{P}^0 \mathfrak{J} + \mathfrak{P}^0 \mathfrak{J} + 2\text{Re}[\mathfrak{S}^0 S^0]) c_{23}^2 s_{23}^2; \quad (\text{A } 35)$$

$$D = 2\text{Re}[\mathfrak{S}^0 S^0] c_{23}^2 s_{23}^2; \quad (\text{A } 36)$$

$$E = 2\text{Im}[\mathfrak{S}^0 S^0] c_{23}^2 s_{23}^2; \quad (\text{A } 37)$$

$$P(\nu_\mu \rightarrow \nu_\tau) = A \cos \delta + B \sin \delta + C + D \cos 2\delta + E \sin 2\delta; \quad (\text{A } 38)$$

$$A = 2\text{Re}[(S^0 s_{23}^2 + S^0 c_{23}^2) (S^0 + S^0)] c_{23} s_{23}; \quad (\text{A } 39)$$

$$B = 2\text{Im}[(S^0 s_{23}^2 + S^0 c_{23}^2) (S^0 - S^0)] c_{23} s_{23}; \quad (\text{A } 40)$$

$$C = \mathfrak{P}^0 \mathfrak{J} s_{23}^4 + \mathfrak{P}^0 \mathfrak{J} c_{23}^4 + (\mathfrak{P}^0 \mathfrak{J} + \mathfrak{P}^0 \mathfrak{J} + 2\text{Re}[\mathfrak{S}^0 S^0]) c_{23}^2 s_{23}^2; \quad (\text{A } 41)$$

$$D = 2\text{Re}[\mathfrak{S}^0 S^0] c_{23}^2 s_{23}^2; \quad (\text{A } 42)$$

$$E = 2\text{Im}[\mathfrak{S}^0 S^0] c_{23}^2 s_{23}^2; \quad (\text{A } 43)$$

$$P(\nu_\tau \rightarrow \nu_\tau) = A \cos \delta + B \sin \delta + C + D \cos 2\delta + E \sin 2\delta; \quad (\text{A } 44)$$

$$A = 2\text{Re}[(S^0 - S^0) (S^0 c_{23}^2 - S^0 s_{23}^2)] c_{23} s_{23}; \quad (\text{A } 45)$$

$$B = 2\text{Im}[(S^0 - S^0) (S^0 c_{23}^2 + S^0 s_{23}^2)] c_{23} s_{23}; \quad (\text{A } 46)$$

$$C = \mathfrak{P}^0 \mathfrak{J} s_{23}^4 + \mathfrak{P}^0 \mathfrak{J} c_{23}^4 + (\mathfrak{P}^0 \mathfrak{J} + \mathfrak{P}^0 \mathfrak{J} - 2\text{Re}[\mathfrak{S}^0 S^0]) c_{23}^2 s_{23}^2; \quad (\text{A } 47)$$

$$D = 2\text{Re}[\mathfrak{S}^0 S^0] c_{23}^2 s_{23}^2; \quad (\text{A } 48)$$

$$E = 2\text{Im}[\mathfrak{S}^0 S^0] c_{23}^2 s_{23}^2; \quad (\text{A } 49)$$

References

- [1] Z. Maki, M. Nakagawa and S. Sakata, *Prog. Theor. Phys.* 28 (1962) 870.
- [2] Super-Kamiokande Collaboration, Y. Ashie et al., *Phys. Rev. Lett.* 93 (2004) 101801.
- [3] KamLAND Collaboration, hep-ex/0406035.
- [4] K2K Collaboration: E. A. Liu, et al., hep-ex/0411038.
- [5] V. Barger, et al., *Phys. Rev. Lett.* 82 (1999) 2640.
- [6] E. Lisi, et al., *Phys. Rev. Lett.* 85 (2000) 1166.
- [7] S. P. Mikheev and A. Yu. Smirnov, *Sov. J. Nucl. Phys.* 42 (1985) 913; L. Wolfenstein, *Phys. Rev. D* 17 (1978) 2369.
- [8] Super-Kamiokande Collaboration, Y. Fukuda et al., *Phys. Rev. Lett.* 82 (1999) 1810; *ibid.*, 82 (1999) 2430.

- [9] SNO Collaboration, Q. R. Ahmad et al, Phys. Rev. Lett. 89 (2002) 011301; *ibid.*, Phys. Rev. Lett. 89 (2002) 011302.
- [10] KamLAND Collaboration, K. Eguchi et al, Phys. Rev. Lett. 90 (2003) 021802.
- [11] SuperKamokande Collaboration, Y. Fukuda et al, Phys. Rev. Lett. 82 (1999) 2644; *ibid.*, Phys. Lett. B 467 (1999) 185.
- [12] CHOOZ Collaboration, M. Apollonio et al, Phys. Lett. B 466 (1999) 415.
- [13] Belle Collaboration, K. Abe et al, Phys. Rev. Lett. 87 (2001) 091802; BABAR Collaboration, B. Aubert et al, Phys. Rev. Lett. 87 (2001) 241801.
- [14] A. Cohen, D. Kaplan, A. Nelson, Ann. Rev. Nucl. Part. Sci. 43 (1993) 27.
- [15] M. Fukugita and T. Yanagita, Phys. Lett. B 174 (1986) 45.
- [16] Y. Itow et al, KEK report 2001-4, ICRR-report-477-2001-7, TRIP-01-05, hep-ex/0106019; BNL Neutrino Working Group: M. Dwan et al. BNL-69395, hep-ex/0211001.
- [17] S. Geer, Phys. Rev. D 57 (1998) 6989; Erratum *ibid.* D 59 (1999) 039903. C. Albright et al, Fermilab-fn-692, hep-ex/0008064; R. Raju et al, FNAL-CONF-01/226-E, hep-ex/0108041.
- [18] J. Arif M. Koike and J. Sato, Phys. Rev. D 56 (1997) 3093; J. Arif and J. Sato, Phys. Rev. D 61 (2000) 073012.
- [19] O. Yasuda, Acta Phys. Polon. B 30 (1999) 3089.
- [20] M. Koike and J. Sato, Phys. Rev. D 62 (2000) 073006.
- [21] J. Sato, Nucl. Instrum. Meth. A 472 (2000) 434.
- [22] H. Minakata and H. Nunokawa, Phys. Lett. B 495 (2000) 369.
- [23] M. Koike and J. Sato Mod. Phys. Lett. A 14 (1999) 1297.
- [24] T. Ota and J. Sato, Phys. Rev. D 63 (2001) 093004.
- [25] T. Miura et al, Phys. Rev. D 64 (2001) 073017.
- [26] T. Miura et al, Phys. Rev. D 64 (2001) 013002.
- [27] E. Kh. Akhmedov et al, Nucl. Phys. B 608 (2001) 394.
- [28] A. Cervera et al, Nucl. Phys. B 579 (2000) 17; Erratum *ibid.* B 593 (2001) 731.
- [29] M. Freund, Phys. Rev. D 64 (2001) 053003.
- [30] E. Kh. Akhmedov et al, hep-ph/0402175.
- [31] V. Naumov, Int. J. Mod. Phys. D 1 (1992) 379
- [32] P. F. Harrison and W. G. Scott, Phys. Lett. B 476 (2000) 349.
- [33] S. J. Parke and T. J. Weiler Phys. Lett. B 501 (2001) 106.
- [34] H. Minakata and H. Nunokawa, JHEP 0110 (2001) 001.
- [35] O. Yasuda, Phys. Lett. B 516 (2001) 111.
- [36] P. Lipari, Phys. Rev. D 64 (2001) 033002.
- [37] J. Pinney and O. Yasuda, Phys. Rev. D 64 (2001) 093008.
- [38] M. Freund, P. Huber, M. Lindner, Nucl. Phys. B 615 (2001) 331.
- [39] H. Yokomakura, K. Kinura and A. Takamura, Phys. Lett. B 544 (2002) 286.

- [40] K. Kinoshita, A. Takahara and H. Yokoyama, *Phys. Lett. B* 537 (2002) 86; *Phys. Rev. D* 66 (2002) 073005; *J. Phys. G* 29 (2003) 1839.
- [41] H. Yokoyama, K. Kinoshita and A. Takahara, *Phys. Lett. B* 496 (2000) 175.
- [42] A. Takahara, K. Kinoshita and H. Yokoyama, *Phys. Lett. B* 595 (2004) 414.
- [43] K. Kinoshita, A. Takahara and H. Yokoyama, *Phys. Lett. B* 600 (2004) 91.
- [44] V. Barone, K. W. Kim, S. Pakvasa, R. Phillips, *Phys. Rev. D* 22 (1980) 2718
- [45] S. Choubey, P. Roy, *Phys. Rev. Lett.* 93 (2004) 021803.
- [46] R. Gandhi, P. Ghoshal, S. Goswami et al., [hep-ph/0408361](#); [hep-ph/0411252](#)
- [47] D. Choudhury, A. Datta, [hep-ph/0410266](#);
- [48] P. Huber, M. Lindner, W. Winter, *Nucl. Phys. B* 645 (2002) 3.
- [49] P. Huber, M. Lindner, W. Winter, [hep-ph/0412199](#).
- [50] L. Shan, Y. Wang, C. Yang, X. Zhang, F. Liu, B. Young, *Phys. Rev. D* 68 (2003) 013002.